Design of an Advanced Portable System for High Density Surface EMG Recording with Wireless Control of Signal Quality

5

Physiological Applications of the System

5.1 General

This section describes two physiological applications using the multi-channel HD-sEMG recording system with wireless communication (HD-sEMG RSWC) prototype.

In the first application, EMG signals are acquired from the subject's biceps brachii and single differential EMG signals along muscle fiber direction column by column (7 single differential signals per column) are plotted. Motor unit action potential (MUAP) produced by motor units of biceps brachii is detected with an inter-electrode distance (IED) of 1cm. Information concerning the innervation zone (IZ) and conduction velocity of the MUAP can be obtained from all columns showing the MUAP. The propagation of MUAPs is along muscle fiber direction. Location of the IZ is estimated, by visual inspection. Conduction velocity (CNV) is estimated as the ratio between the distance D travelled by the MUAP in the time interval T.

In the second application, EMG signals are acquired by placing 64-channel electrodes grid (IED=1cm) on the proximal portion of dorsal forearm of subjects. Spatial distribution of surface EMG amplitude on the forearm is used to estimate the most active muscle area during the following specific biomechanical actions, including: wrist extension (WRIST EXT), ulnar deviation (ULN DEV), middle finger extension (MID), ring finger extension (RING) and little finger extension (LIT). Whether spatial properties of monopolar EMG amplitude distribution (RMS) over the proximal portion of dorsal forearm can be used to discriminate different contractions or not is studied and the results is presented in **SECTION5.3.7.**

5.2 Application 1: Analysis of EMG Signals Acquired from Biceps Brachii Muscle

5.2.1 Background

High Density sEMG (HD-sEMG) applies a linear 2D surface electrode array placed along the muscle fibers detects motor unit action potentials (MUAPs) propagating bilaterally to the tendons. The location of the propagation source is presumed to mark as an innervation zone (IZ) [1]. Biceps brachii is a two headed muscle located superficially on the upper arm and is considered as a muscle that has better EMG signals. Main action of biceps brachii is supination of the forearm. It also flexes the arm at the elbow and at the shoulder. The anatomy of biceps brachii in the upper arm is depicted in **Figure5.1**.

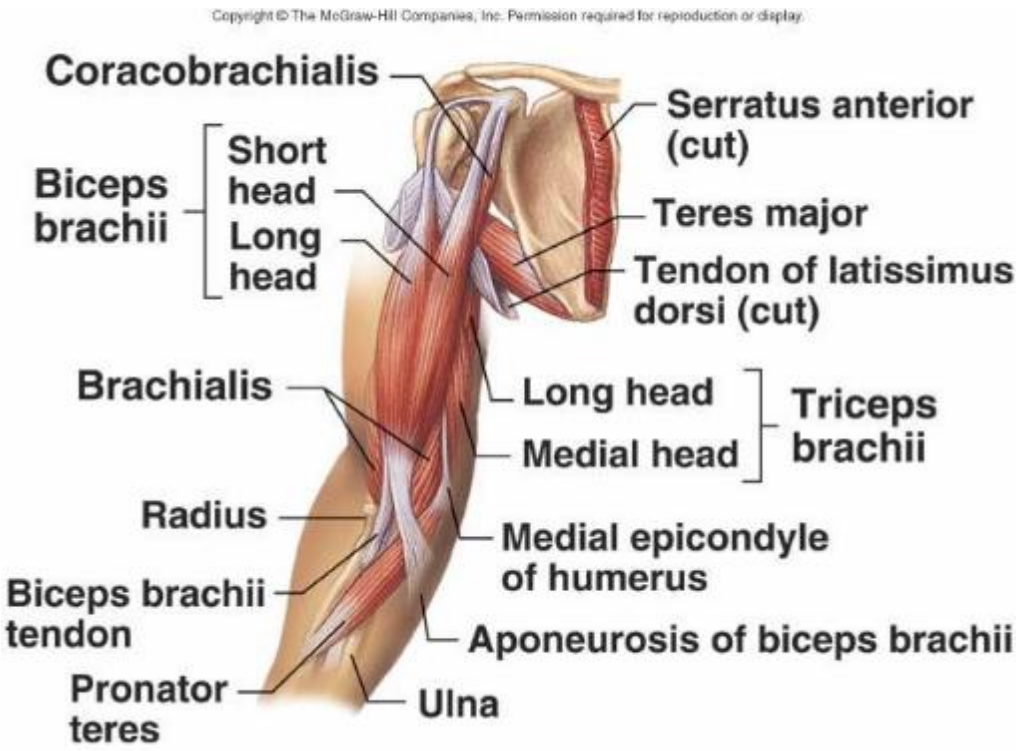

Figure5.1: Anatomy of the upper arm. The muscles of the upper arm are responsible for the flexion and extension of the forearm at the elbow joint. Flexion of the forearm is achieved by a group of three muscles – the brachialis, biceps brachii, and brachioradialis. These flexor muscles are all located on the anterior side of the upper arm and extend from the humerus and scapula to the ulna and radius of the forearm. Additionally, the biceps brachii operates as a supinator of the forearm by rotating the radius and moving the palm of the hand anteriorly. On the posterior side of the upper arm is the triceps brachii, which acts as an extensor of the forearm at the elbow and the humerus at the shoulder. The triceps brachii, as its name indicates, has three heads whose origins are on the scapula and humerus. These three heads merge to insert on the olecranon of the ulna [2].

5.2.2 Experiment Protocol

5.2.2.1 Muscle of Interest

Muscle of interest in this study is biceps brachii (see **Figure5.10**). It is a two headed muscle located superficially on the upper arm and is considered as a muscle that easy to detect propagation of motor unit action potential (MUAP).

5.2.2.2 Devices and Instruments

Devices and instruments that used in the measurements include: a grid of sixty-four electrodes organized in a 8x8 matrix with 10 mm inter electrode distance (IED), a prototype of the multi-channel HD-sEMG recording system with wireless communication (HD-sEMG RSWC), an access point, a laptop, abrasive paste, alcohol (for cleaning the surface skin), reference electrodes and cables.

5.2.2.3 Placement of Electrode Grid

A sixty-four electrode grid is placed to cover a skin portion (located from 10% to 38%) of the upper arm length (measured from the elbow to the shoulder), as presented in **Figure5.2**. The average upper arm length of participated subjects is 29 cm, 10% corresponds to 3 cm and 38% corresponds to 11cm (measured start from elbow side).

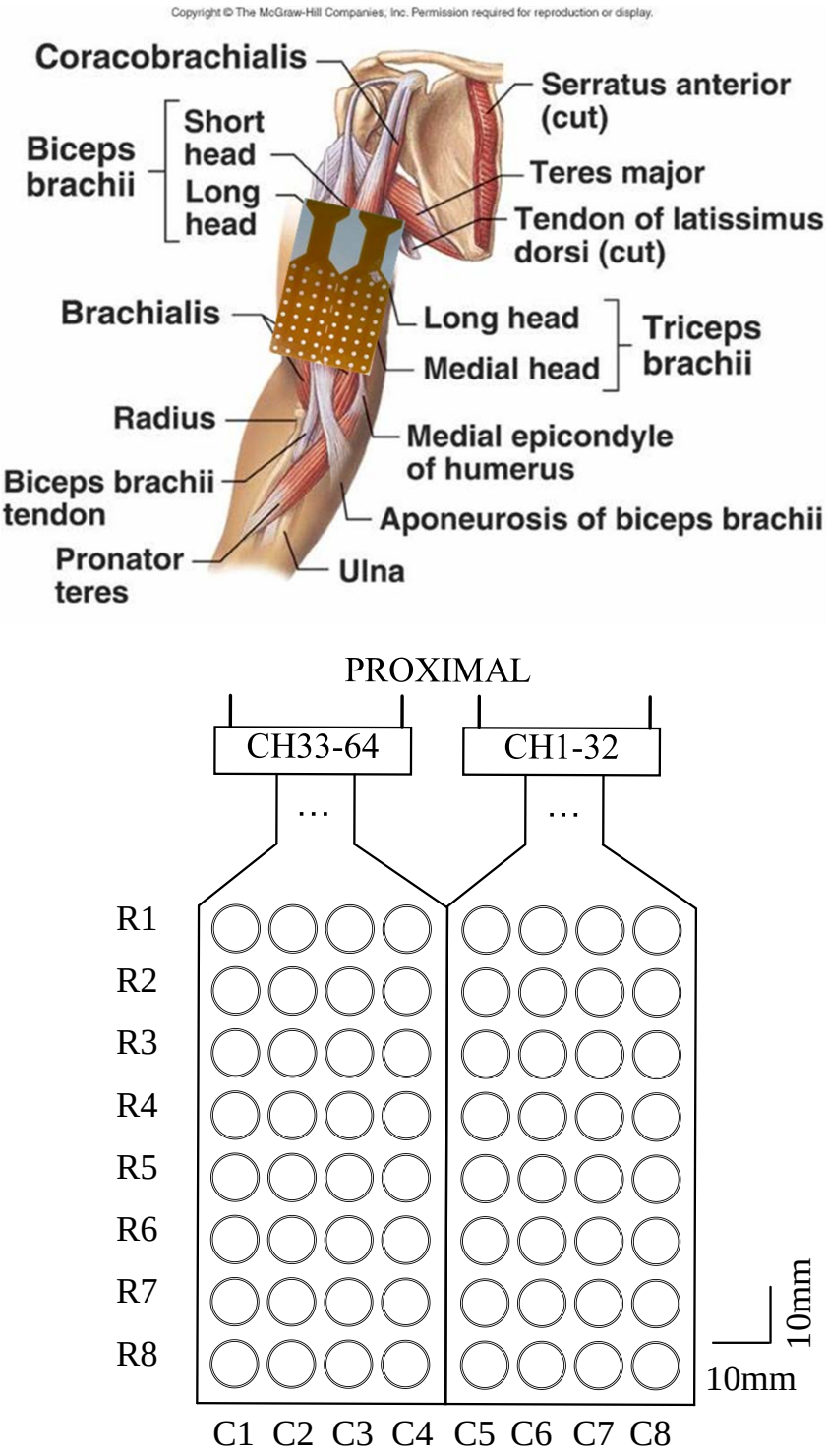

Figure5.2: Placement of 64-channel (8x8) electrodes array on the surface of the subject's biceps brachii along muscle fiber direction. The IEDs of the electrodes are 10mm. The average upper arm length of participated subjects is 29 cm, 10% corresponds to 3 cm and 38% corresponds to 11cm (measured start from elbow side).

5.2.3 Experiment Connections

Connections between the subjects and the prototype of multi-channel HD-sEMG recording system with wireless communication (HD-sEMG RSWC) are depicted in **Figure5.3**.

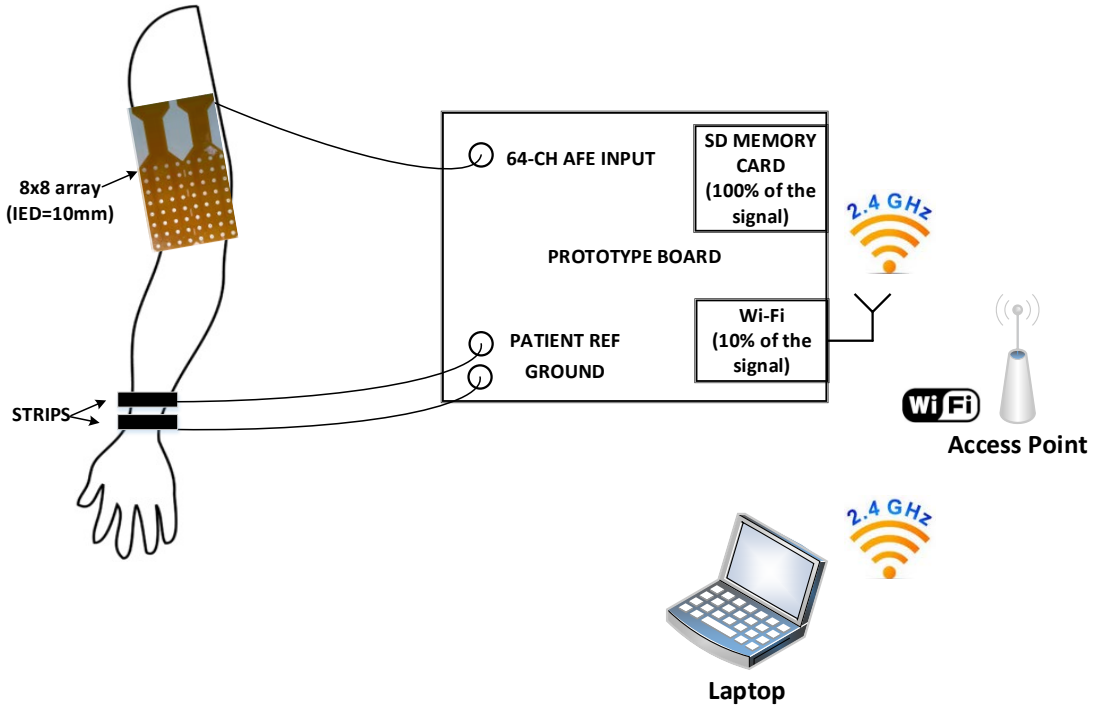

Figure5.3: Connections between the subject and the prototype of multi-channel HD-sEMG recording system with wireless communication. During the measurements, a grid of sixty-four electrodes (8x8, 10mm IED) is placed on the the surface of the subject's biceps brachii along muscle fiber direction and is connected to the on-board 64-channel AFE (Analog Front End) inputs, while two strips (wetted) are also placed on the wrist separated from each other as references (patient reference and ground). The prototype is linked with an access point wireless (radio at 2.4GHz with Wi-Fi). Sampled data are stored in a micro-SD memory card, meanwhile, a subset of 1/10th of every second (first 100ms) are transmitted to a stand-alone Wi-Fi module. A laptop (with on-line visualizing software installed) is linked with the same access point and is used for on-line visualization to check signals quality.

5.2.4 Experiment Procedures

Before the beginning of the experimental session, the subjects (two subjects, one female and one male) were allowed to familiarize with the experimental setup and with the tasks required for the experimental protocol. The treatment of the skin and the placement of electrodes followed the European SENIAM (Surface EMG for a Non-Invasive Assessment of Muscles) standard [3]. During acquisition, two subjects are asked to sit down with back on the chair and hold 3kg weight with their palm up for 5 seconds, as presented in **Figure5.4**.

Figure5.4: Position and task of the subject during HD-sEMG acquisition. The subject was asked to sit down with back on the chair and hold 3kg weight with her palm up without touch the leg for 5 seconds.

5.2.5 Results and Discussions

Table 5.1 presents the information of the two subjects who participated in our measurements.

Table5.1: Information about the two subjects who participated in the measurement. All two subjects are dextromanuality (right-handed) and the forearm in this table refers to right forearm.

Subject	Gender	Age [year]	Height [cm]	Weight [kg]	Upper-arm Length [cm]
S1	Male	32	170	63	29
S2	Female	22	170	60	29

EMG signals acquired by the prototype of multi-channel HD-sEMG recording system with wireless communication were analysed with MATLAB (version 2010a). EMG signals were acquired during 5s of isometric contractions and were recorded in SD memory for off-line signal processing. These off-line signal processing (were described in **SETCTION4.2-4.4** in detail), includes:

1) DC Removal, the DC offsets were removed from each signal after channel remapping.

2) A 2nd order digital Butterworth zero-lag band-pass (around [20, 500] Hz) filter was performed to remove the noises outside surface EMG bandwidth.

3) If 50Hz power line interference and its harmonics were detected using spectral analysis, an approach called spectrum interpolation was performed to reduce the power line interference and its harmonics (up to 10th harmonics as descried in **SECTION4.4**).

4) EMG signals (monopolar) inside the epoch [1s, 4s] were extracted.

5) Single differential EMG signals along muscle fiber direction column by column (7 single differential signals per column) were plotted.

A motor unit (MU) consists of an α-motoneuron in the spinal cord and the muscle fibers it innervates [4]. The α-motoneuron is the final point of summation for all the

descending and reflex input. The number of MUs per muscle in humans may range from about 100 for a small hand muscle to 1000 or more for large limb muscles. A single MU activation is indicated as a “discharging” or “firing” and it generates a “motor unit action potential” (MUAP), which is the sum of the contributions provided by the individual fibers that make up the MU [5]. The neuromuscular junctions (NMJs) of the fibers of a MUC are usually grouped in a narrow region described as the “innervation zone” (IZ), which is often (but not always) in the central part of the MU.

Examples of signals acquired during the same position presented in **Figure5.4** but without holding any weight are presented in **Figure5.5**. Anatomical model consists of bone, muscle tissue, a subcutaneous layer and skin [6][7] are used to explain the phenomena detected in **Figure5.5**.

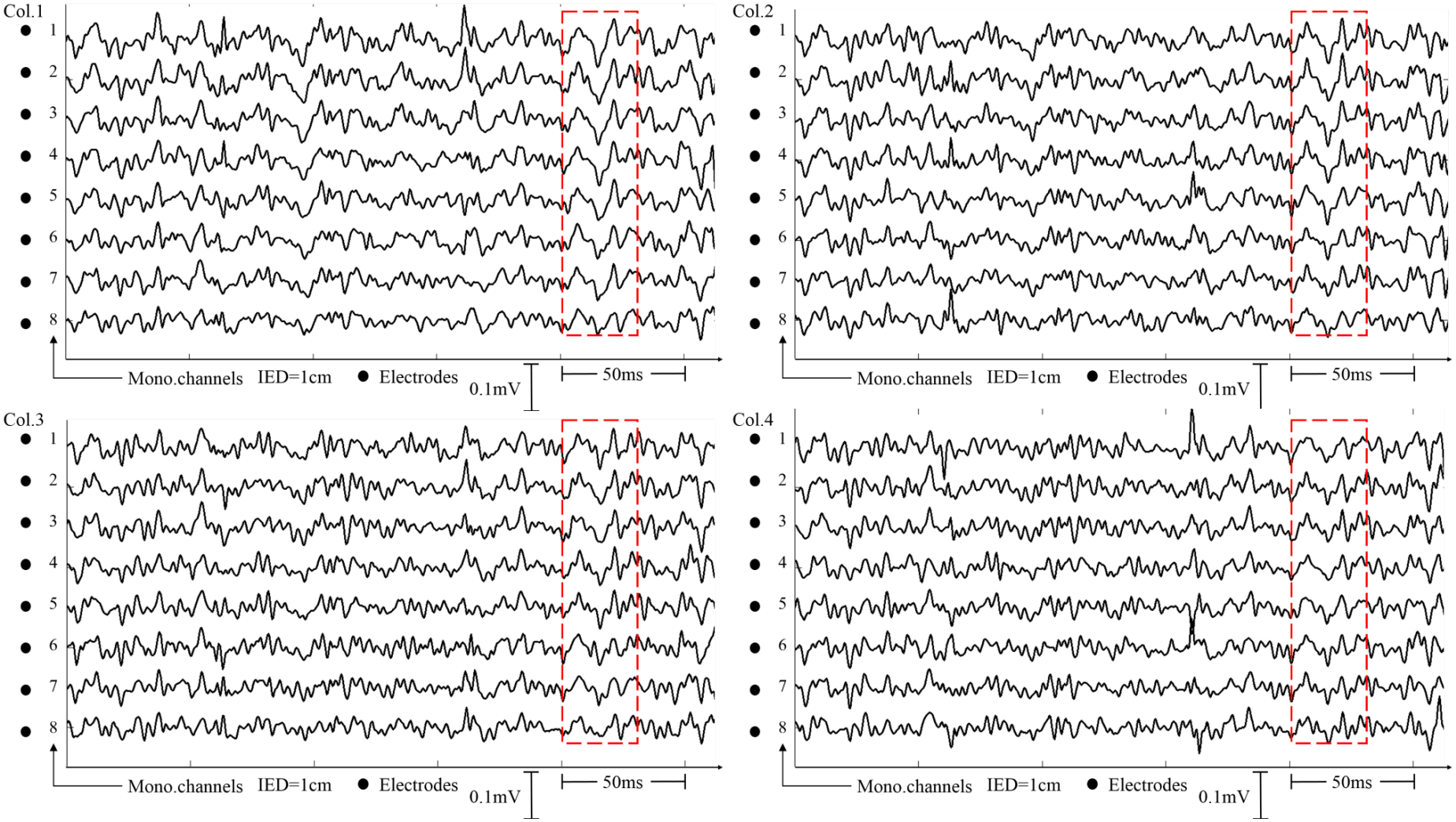
Col.1
1
2
3
4
5
6
7
8
Mono.channels IED=1cm Electrodes
0.1mV
50ms
Col.2
1
2
3
4
5
6
7
8
Mono.channels IED=1cm Electrodes
0.1mV
50ms
Col.3
1
2
3
4
5
6
7
8
Mono.channels IED=1cm Electrodes
0.1mV
50ms
Col.4
1
2
3
4
5
6
7
8
Mono.channels IED=1cm Electrodes
0.1mV
50ms

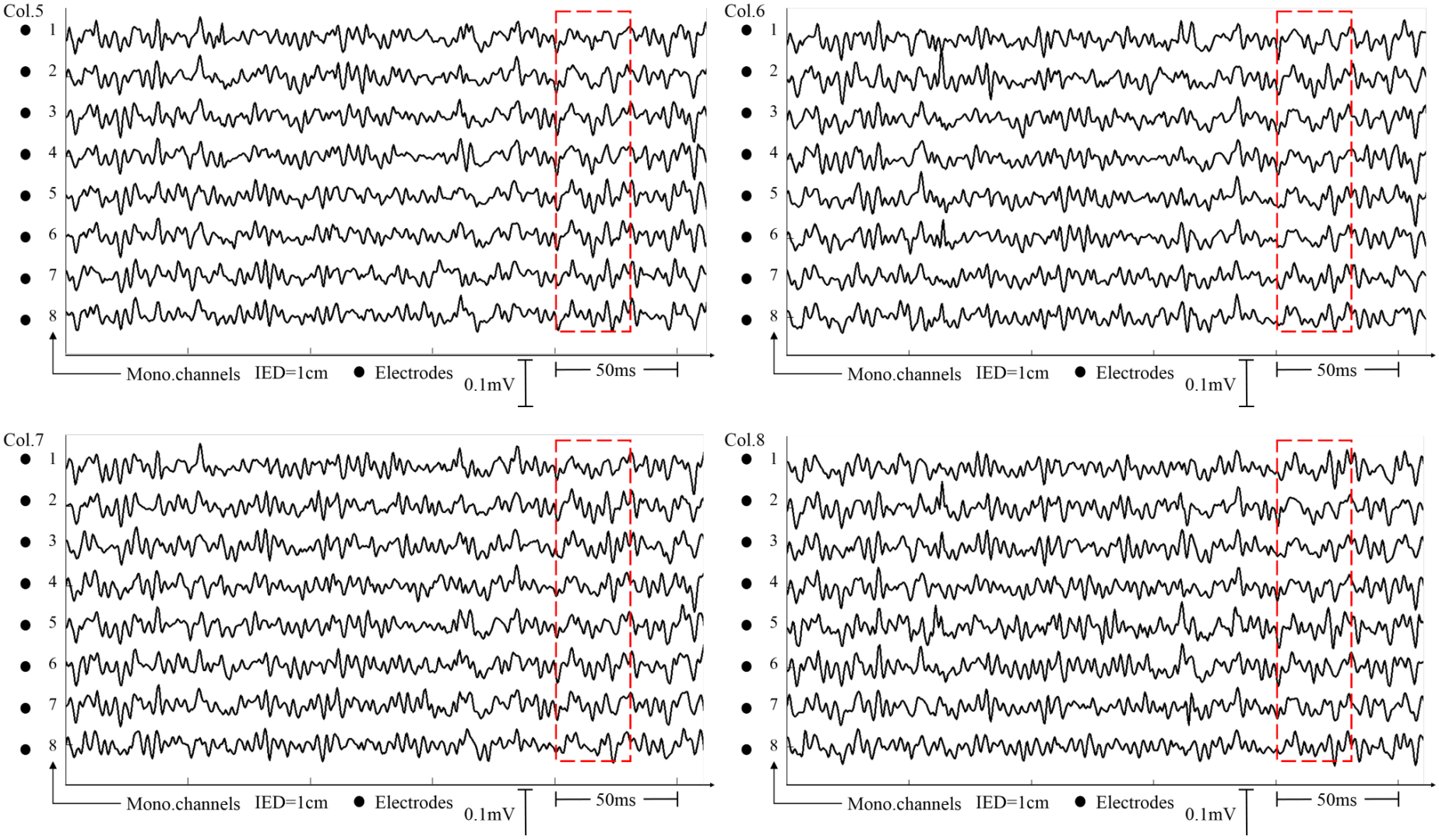
Col.5
1
2
3
4
5
6
7
8
Mono.channels
IED=1cm
Electrodes
0.1mV
50ms
Col.6
1
2
3
4
5
6
7
8
Mono.channels
IED=1cm
Electrodes
0.1mV
50ms
Col.7
1
2
3
4
5
6
7
8
Mono.channels
IED=1cm
Electrodes
0.1mV
50ms
Col.8
1
2
3
4
5
6
7
8
Mono.channels
IED=1cm
Electrodes
0.1mV
50ms

Figure5.5: Signals detected by a 64-channel electrode grid placed on the subject 1's biceps brachii during the same position presented in Figure5.4 but without holding any weight. Placement of the 64-channel electrode grid is presented in Figure5.2. C1 is column 1 of the electrode grid at lateral end, C8 is column 8 of the electrode grid at medial end. The signals acquired during low level isometric condition is dominant by noise and electrode-gel-skin interface. As presented in this figure, the distributions of noise and electrode-gel-skin interface in 8 different columns are more or less unique. The amplitude of signals acquired (marked in red dashed rectangle) from a MU in the same time appears different, since the distance between the source (MU) and each column is different. The amplitude of signals in column 1-3 are higher than other columns, which is also explained by an anatomical model presented in Figure5.6.

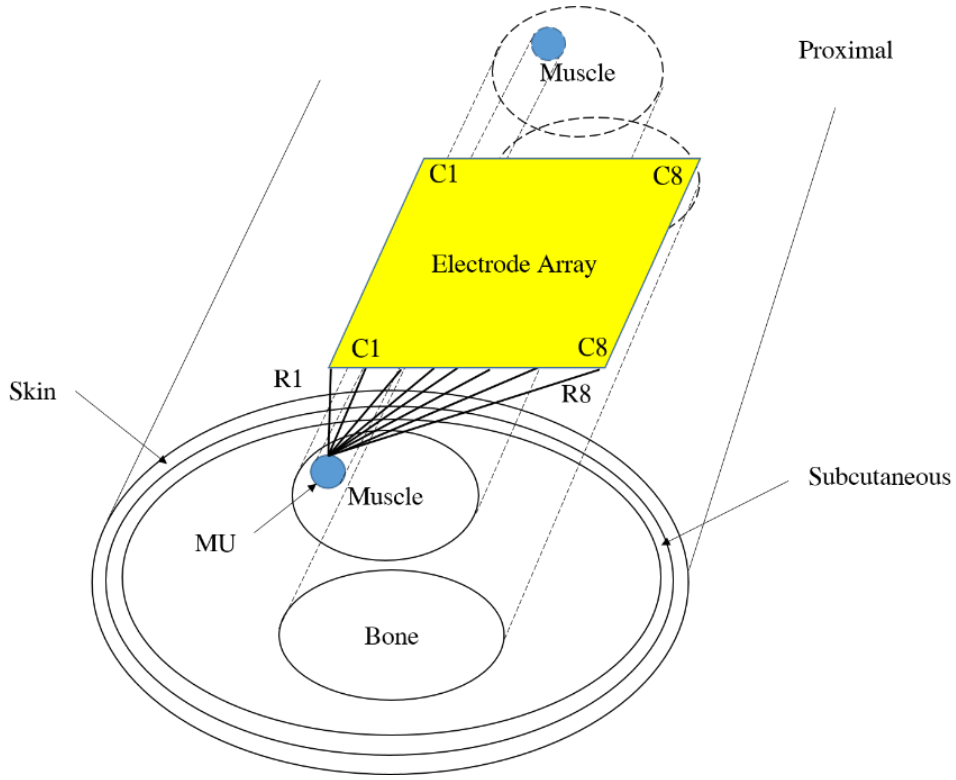

Figure5.6: Anatomical model to explain the phenomena detected in Figure5.5. The model consists of bone, muscle tissue, a subcutaneous layer and skin while MU is simplified as several cylindrical muscle fibers cluster. The source of EMG signals is a MU closer to column 1-3 than other columns of the electrode array placed on the surface of skin. C1 is column 1 and C8 is column 8 of the electrode array. R1 is the distance between MU and C1. R8 is the distance between MU and C8.

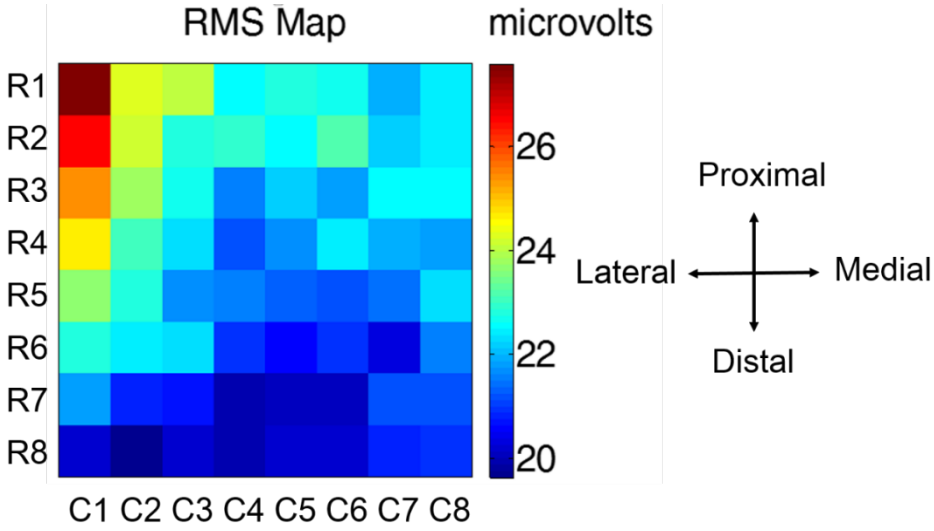

Figure5.7: RMS amplitude of monopolar signals detected by a 64-channel electrode grid placed on the subject 1's biceps brachii during the same position presented in Figure5.4 but without holding any weight. As presented in this figure, the distributions of noise and electrode-gel-skin interface in 8 different columns are more or less unique. The maximal RMS is 28 µV detected at column 1 which has the short distance between the source (MU) and electrodes in column 1 (as shown in Figure5.6)

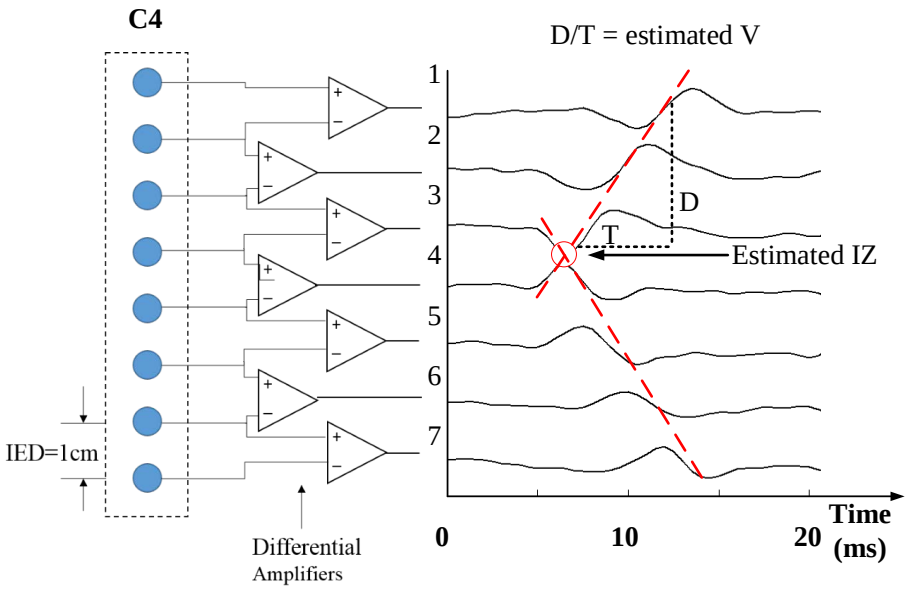

Figure5.8: An example of single differential EMG signals acquired from column 4 of the 64-channel electrode grid (see Figure5.2) of subject 1 (S1) contracting with holding 2kg weight. EMG signals acquired originally were monopolar and were converted to single differential by software. Motor unit action potential (MUAP) produced by motor units of biceps brachii is detected with an inter-electrode distance (IED) of 1cm. Information concerning the innervation zone (IZ) and conduction velocity of the MUAP can be obtained from the 7 signals.

The red lines indicate the propagation of the MUAP along muscle fiber direction. The location of the IZ is estimated, by visual inspection, under electrode 4. Conduction velocity (CNV) is estimated by visually estimated as the ratio between the distance D and the time interval T. The estimated CNV in this figure is 3.75 m/s (D=30mm and T=8ms).

As shown in **Figure5.8**, propagation of MUAPs is along muscle fiber direction. The location of the propagation source is presumed to mark as an innervation zone (IZ). Location of the IZ is estimated, by visual inspection. Conduction velocity (CNV) is estimated as the ratio between the distance D travelled by the MUAP in the time interval T. A 250ms epoch of single differential EMG signals detected from a 64-channel electrode grid placed on the biceps brachii of subject 1 and subject 2during hold 3kg weight isometric condition is presented in **Figure5.9** and **Figure5.11**.

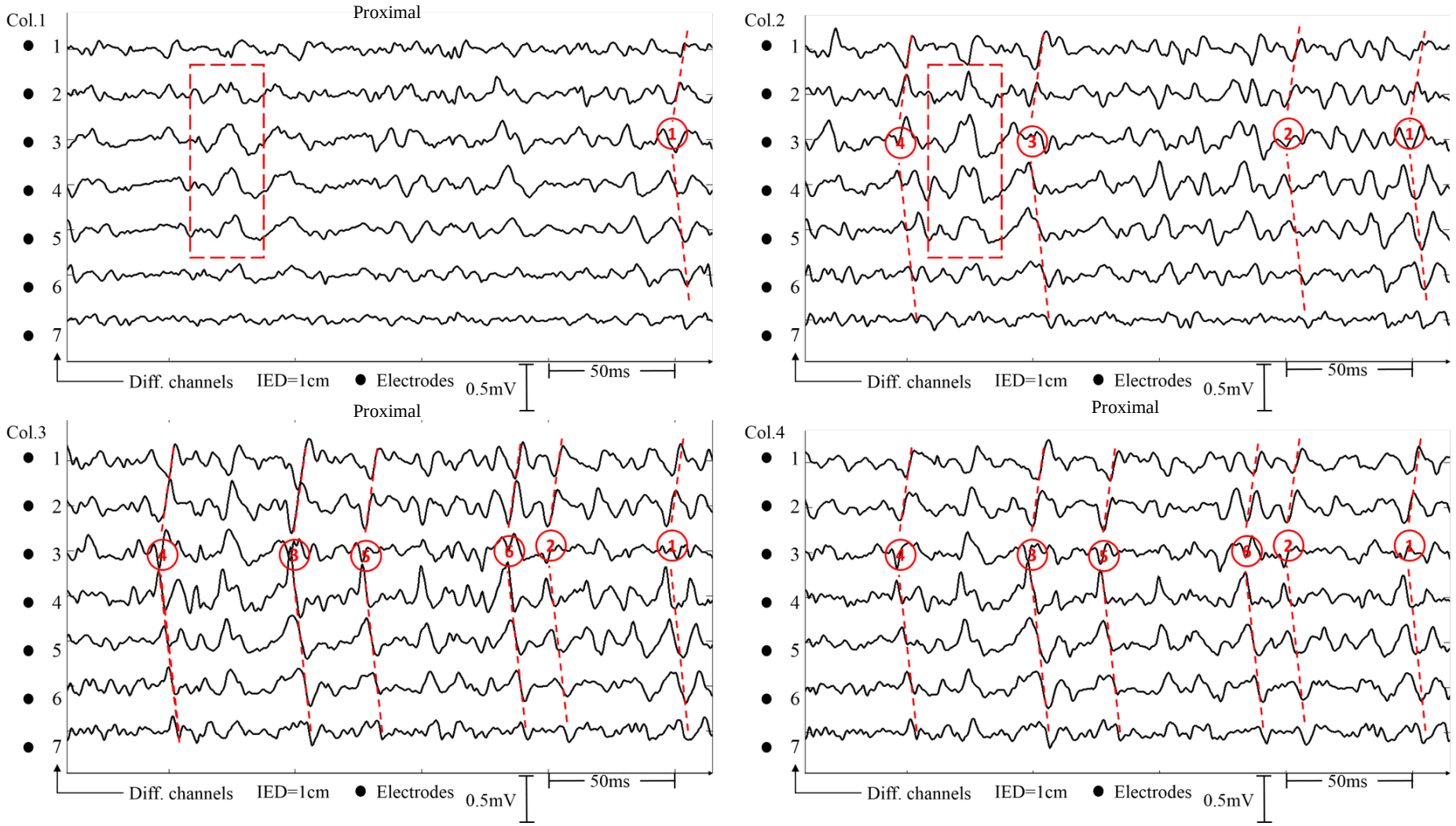
Col.1
Proximal
1
2
3
4
5
6
7
Diff. channels
IED=1cm
Electrodes
0.5mV
50ms
Col.2
Proximal
Col.3
Proximal
Col.4
Proximal

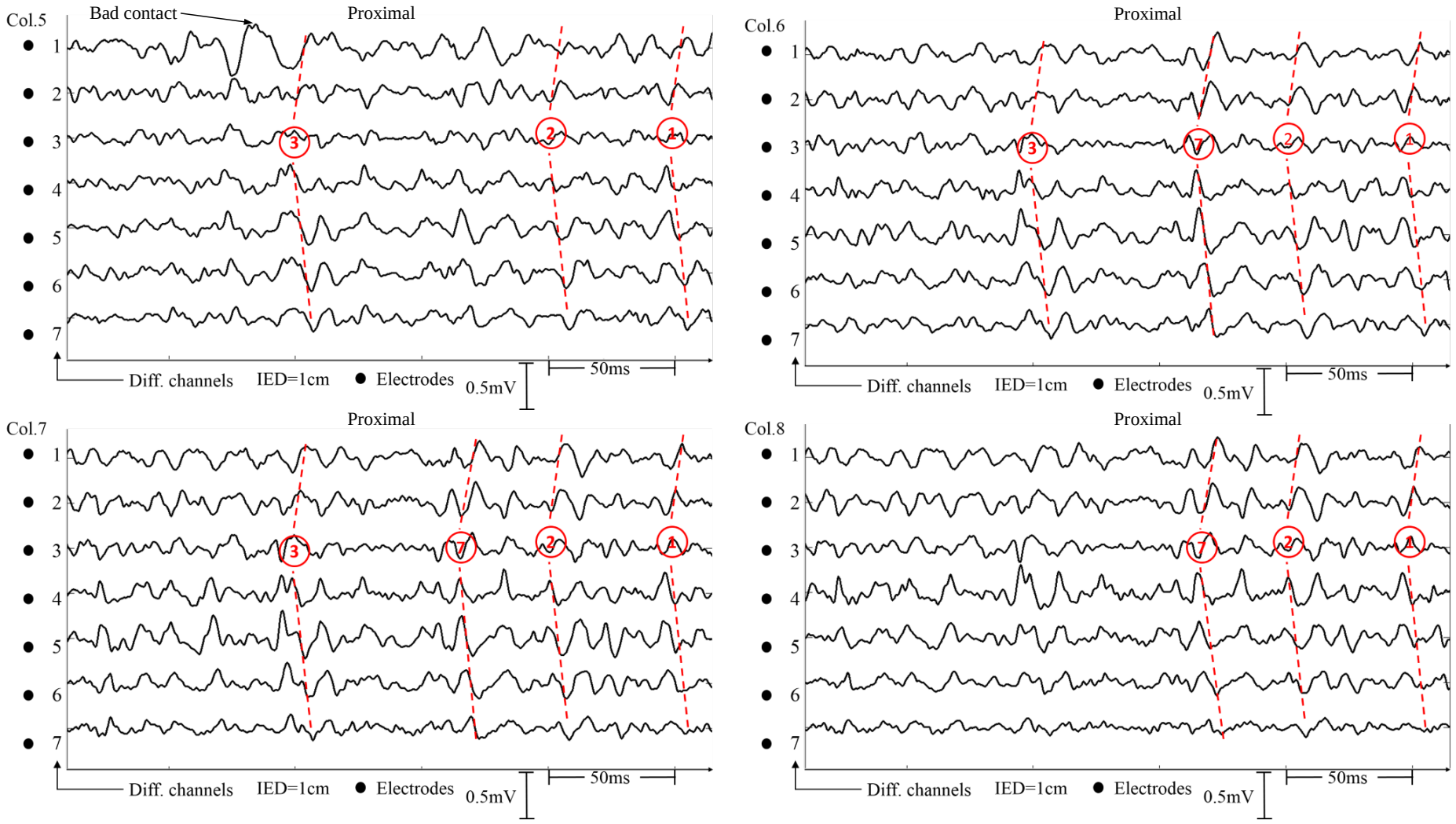
Col.5
Bad contact
Proximal
1
2
3
4
5
6
7
Diff. channels
IED=1cm
Electrodes
0.5mV
50ms
Col.6
Proximal
Col.7
Proximal
Col.8
Proximal

Figure5.9: Time course (over 250ms) of the longitudinal single differential (LSD) EMG signals detected from each column (columns 1-8, 7 channels per column). By visual analysis, the innervation zone is detected under rows 3-4. The LSD signals are sampled at 2000 S/s (0.5ms between samples). A 64-channel electrode grid (see Figure5.2) is placed on the biceps brachii of subject 1 holding 3kg weight in isometric condition. EMG signals are initially acquired in monopolar configuration and are converted to SD later. The propagation of MUAPs is marked with red line. Different MUs are also marked with number in a circle. The anatomical model to explain phenomena detected in this figure is presented in Figure5.10. No propagation MU is detected in column 1 and column 2, which is marked with red dashed rectangle. These no propagation MU may be due to cross talk from its neighbour muscle (triceps) or motion artefacts. CNVs estimated (with the method presented in Figure5.7) from each column are more or less the same.

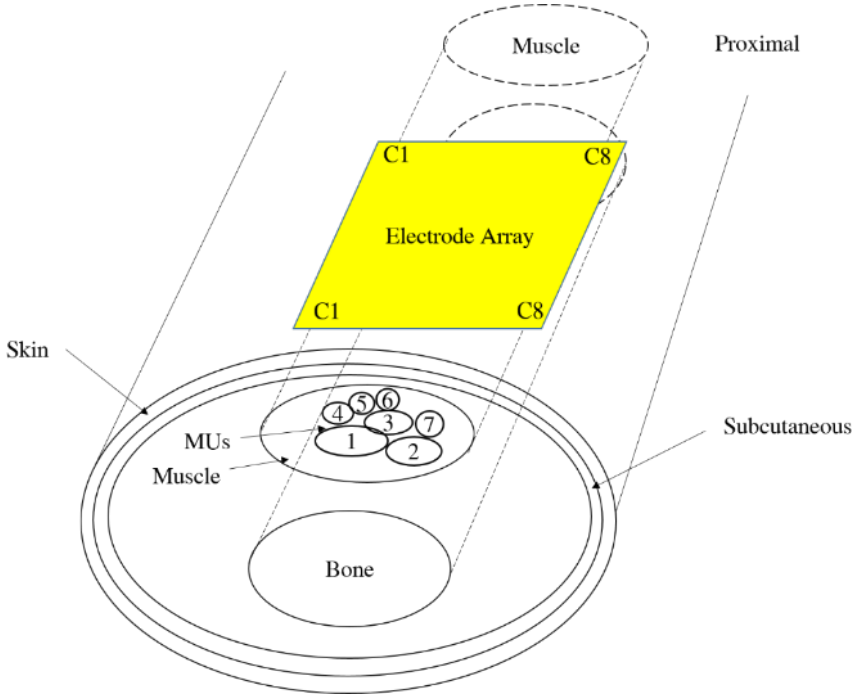

Figure5.10: Anatomical model to explain the phenomenon detected in Figure5.9. The model consists of bone, muscle tissue, a subcutaneous layer and skin while MUs are simplified as several cylindrical muscle fibers cluster marked with number. MU1 (marked with 1) has the largest territory so that can be detected in all columns. MU2 also has a large territory and can be detected in column 2-7. MU 3-7 are small MUs located more superficial to skin and can only be detected in fewer columns of the electrode array. C1 is column 1 and C8 is column 8 of the electrode array.

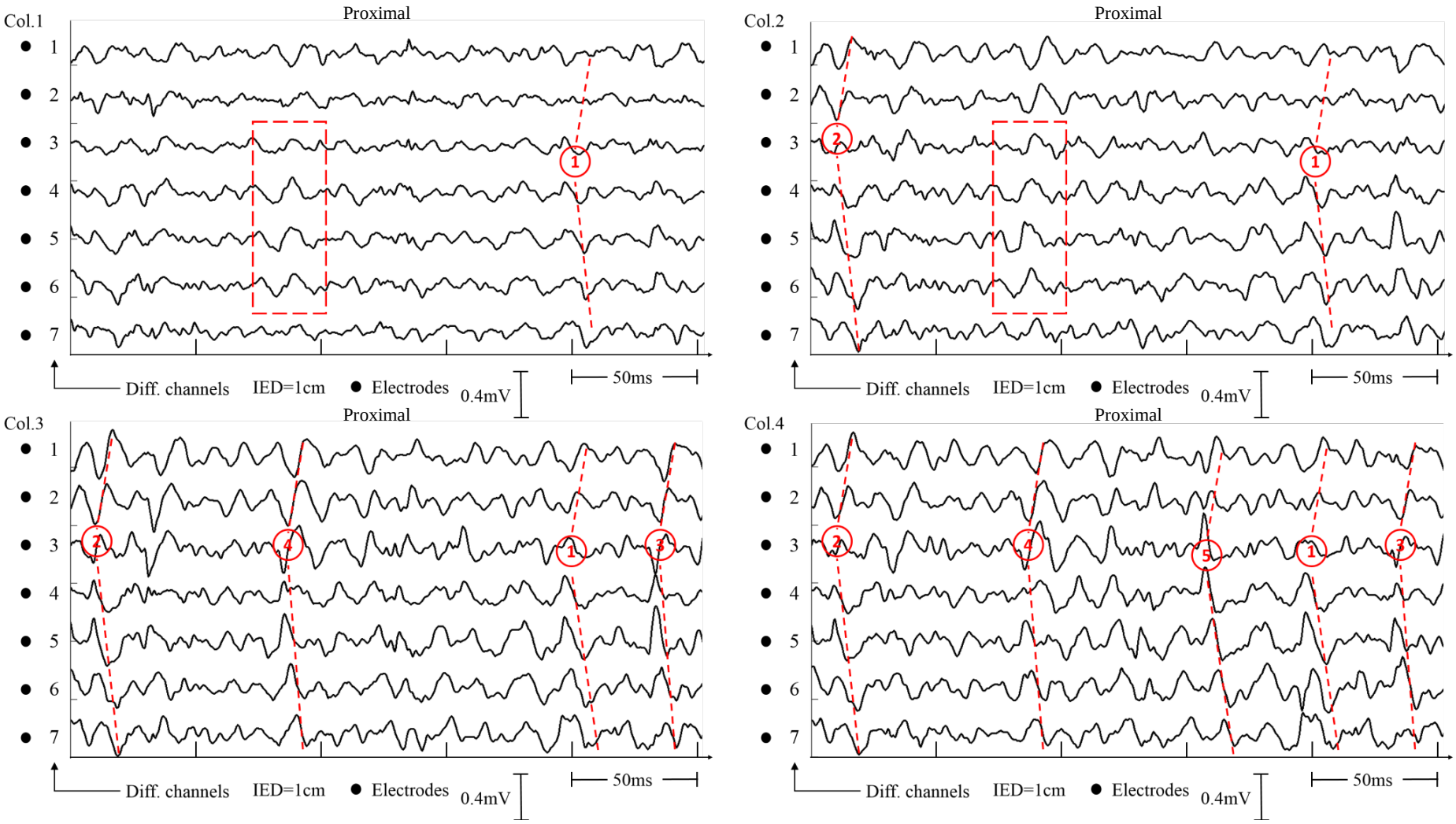
Col.1
Proximal
1
2
3
4
5
6
7
Diff. channels
IED=1cm
Electrodes
0.4mV
50ms
Col.2
Proximal
Col.3
Proximal
Col.4
Proximal

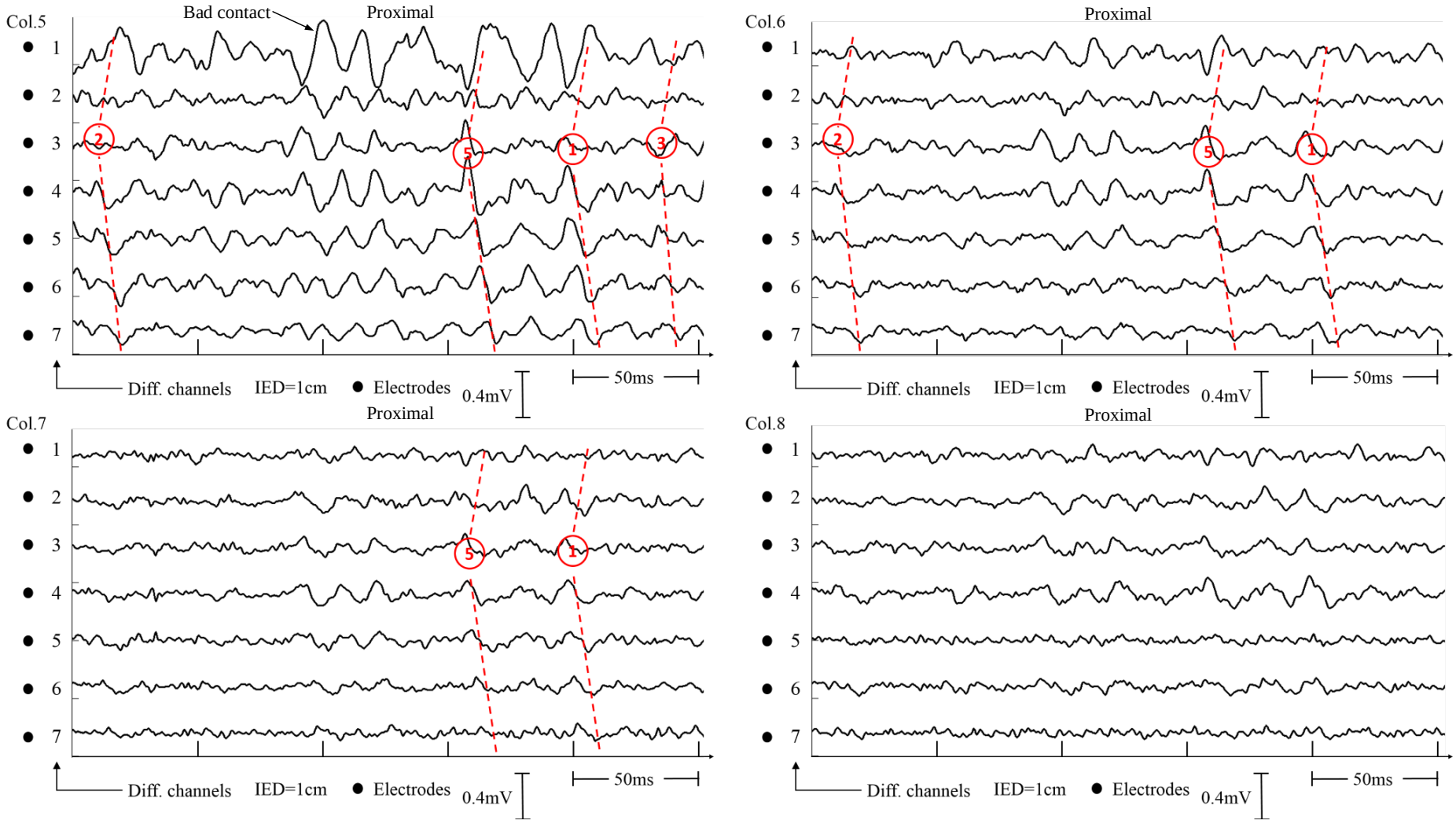
Col.5
Bad contact
Proximal
1
2
3
4
5
6
7
2
5
1
3
Diff. channels
IED=1cm
Electrodes
0.4mV
50ms
Col.6
Proximal
1
2
3
4
5
6
7
2
5
1
Diff. channels
IED=1cm
Electrodes
0.4mV
50ms
Col.7
Proximal
1
2
3
4
5
6
7
5
1
Diff. channels
IED=1cm
Electrodes
0.4mV
50ms
Col.8
Proximal
1
2
3
4
5
6
7
Diff. channels
IED=1cm
Electrodes
0.4mV
50ms

Figure5.11: Time course (over 250ms) of the longitudinal single differential (LSD) EMG signals detected from each column (columns 1-8, 7 channels per column). By visual analysis, innervation zone is detected under rows 3-4. The LSD signals are sampled at 2000 S/s (0.5ms between samples). A 64-channel electrode grid (see Figure5.2) is placed on the biceps brachii of subject 2 holding 3kg weight in isometric condition. EMG signals are initially acquired in monopolar configuration and are convert to SD later. The propagation of MUAPs is marked with red line. Different MUs are also marked with number in a circle. The anatomical model to explain phenomena detected in this figure is presented in Figure5.12. No propagation MU is detected in column 1 and column 2, which is marked with red dashed rectangle. These no propagation MU may be due to cross talk from its neighbour muscle (triceps) or motion artefacts. CNVs estimated (with the method presented in Figure5.7) from each column are more or less the same.

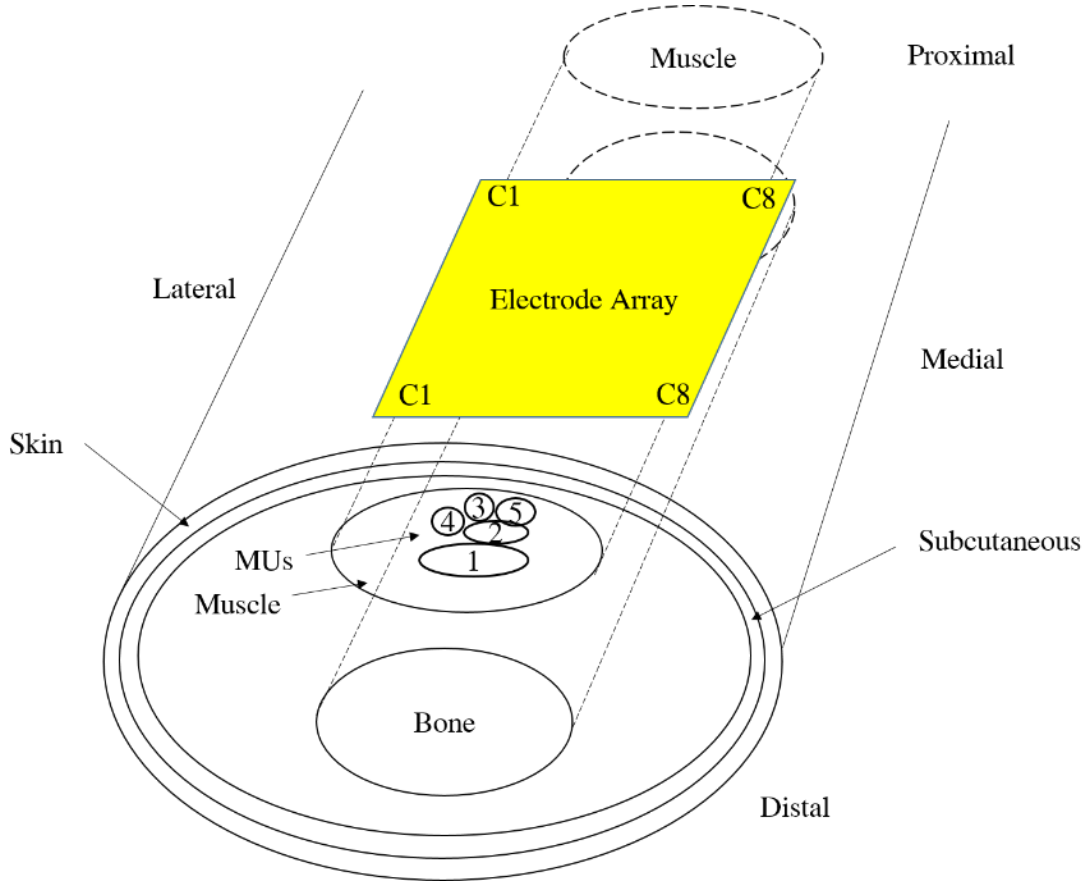

Figure5.12: Anatomical model to explain the phenomenon detected in Figure5.11. The model consists of bone, muscle tissue, a subcutaneous layer and skin while MUs are simplified as several cylindrical muscle fibers cluster marked with number. MU1 (marked with 1) has the largest territory so that can be detected in column 1-7. MU2 also has a large territory and can be detected in column 2-6. MU 3-5 are small MUs located more superficial to skin and can only be detected in fewer columns of the electrode array. C1 is column 1 and C8 is column 8 of the electrode array.

5.3.6 Conclusions

In the first application, information concerning the innervation zone (IZ) and conduction velocity of the MUAP can be obtained from all columns showing the MUAP as described in **Figure5.9** and **Figure5.11**. The propagation of MUAPs is along muscle fiber direction. Location of the IZ is estimated, by visual inspection. Conduction velocity (CNV) is estimated as the ratio between the distance D travelled by the MUAP in the time interval T.

As shown in **Figure5.10**, the territories of different MUs are different in subject 1 both in size and in depth. Only MU1 can be detected in all 8 columns, some MUs (MU2 and MU3) can be detected in more columns (column 2-7) and some MUs (MU5 and MU6) can only be detected in two columns.

As shown in **Figure5.12**, the territories of different MUs are different in subject 2 both in size and in depth. MU1 has the largest territory and can be detected in column 1-7, MU2 can be detected in more columns and the rest MUs (MU 3-5) can only be detected in 2-3 columns.

5.3 Application 2: Spatial Localization of EMG RMS Amplitude Distributions Associated to the Activation of Dorsal Forearm Muscles

5.3.1 Background

5.3.1.1 State of the Art

The study of the degree of independent control of the major extrinsic extensors (extensor digitorum communis, EDC) in [8] indicated that fingers can be selectively extended with a certain degree of independence. Experiments conducted on single motor units of two forearm muscles, extensor carpi radialis (ECR) and extensor digitorum communis (EDC) of human subjects concluded that motor-unit task groups do exist within EDC motoneuron pool [9].

Furthermore, the force study results acquired from strict actions of the human wrist extensors with an electrical neuromuscular stimulation (ENS) method suggest that extensor carpi radialis longus (ECRl) is an abductor and extensor while extensor carpi radialis brevis (ECRb) an extensor rather than an abductor [8]. Other experiments [9] indicated that ECRl is activated more strongly during radial deviation contractions than for wrist extension contractions while ECRb was activated more strongly for extension contractions than for radial deviation contractions.

Human extensor carpi ulnaris (ECU) was found anatomically partitioned and may have up to four partitions by innervation alone or three congruent partitions by innervation and muscle fiber architecture [12].

The results in [13] indicated that specific biomechanical actions [wrist extension (EXT),

ulnar deviation (ULN), middle finger extension (MID), ring finger extension (RING) and little finger extension (LIT)] only activated a relatively small area of the proximal portion of dorsal forearm. The anatomy of muscles in the dorsal compartment of the forearm is depicted in **Figure5.13**.

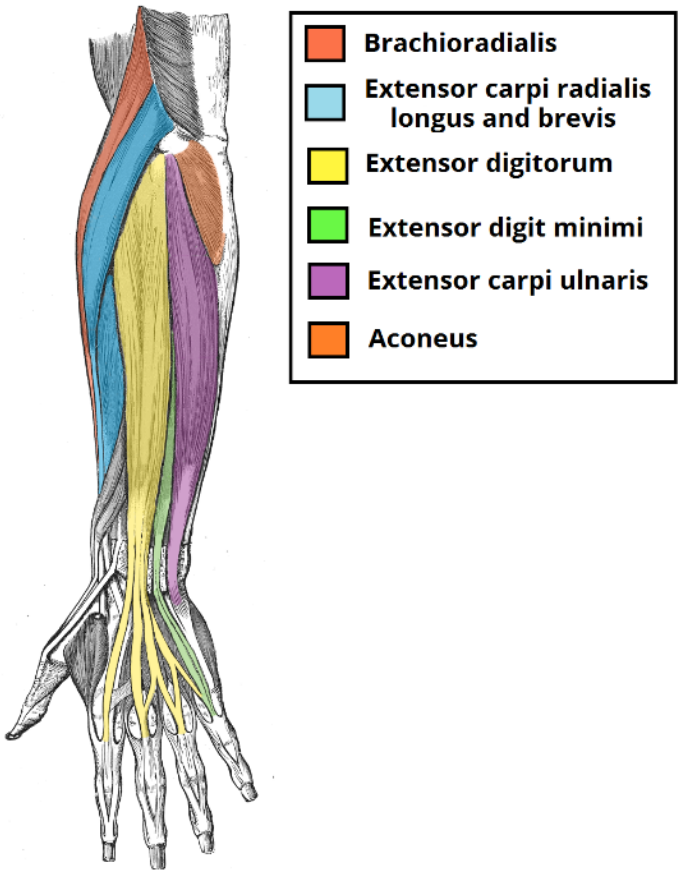

Figure5.13: Muscles in the superficial layer of the posterior forearm, redrawn from [12]. The superficial layer of the posterior forearm contains seven muscles. Brachioradialis (BR) originates from the proximal surface of the supraepicondylar ridge of the humerus, and attaches to the distal end of the radius, just before the radial styloid process. Extensor carpi radialis longus (ECRl) originates from the supracondylar ridge, while extensor carpi radialis brevis (ECRb) originates from the lateral epicondyle. Their tendons attach to metacarpal bones II and III. Extensor digitorum communis (EDC) originates from the lateral epicondyle of the humurus, and attaches to the base of metacarpal V. Extensor carpi ulnaris (ECU) originates from the lateral epicondyle of the humurus, and attaches to the base of metacarpal V. Extensor digiti minimi (EDM) originates from the lateral epicondyle of the humerus. It attaches, with the extensor digitorum tendon, into the extensor hood of the little finger. Aconeus originates from the lateral epicondyle, and attaches to the posterior and lateral part of the olecrannon.

5.3.1.2 Objective of the Physiological Application

In this study we investigated how to use the spatial distribution of surface EMG amplitude acquired by the new multi-channel HD-sEMG recording system with wireless communication (HD-sEMG RSWC) prototype to estimate the most active muscle area during different specific biomechanical actions. These specific biomechanical actions [wrist extension (EXT), ulnar deviation (ULN), middle finger extension (MID), ring finger extension (RING) and little finger extension (LIT)] only activate a relatively small area at the proximal portion of dorsal forearm, according to literature.

5.3.2 Experiment Protocol

5.3.2.1 Muscles of Interest

Muscles of interest in this study are extensor carpi radialis longus (ECRl), extensor carpi radialis brevis (ECRb), extensor digitorum communis (EDC), extensor carpi ulnaris (ECU). These muscles are all located at the dorsal forearm (see **Figure5.13**) and are known as responsible muscles for the following tasks: [wrist extension (EXT), ulnar deviation (ULN), middle finger extension (MID), ring finger extension (RING) and little finger extension (LIT)].

5.3.2.2 Devices and Instruments

Devices and instruments that were used in the measurements include: a grid of sixty-four electrodes organized in a 8x8 matrix with 10 mm inter electrode distance (IED), a prototype of the multi-channel HD-sEMG recording system with wireless communication (HD-sEMG RSWC), an access point, a laptop, abrasive paste, alcohol (for cleaning the surface skin), reference electrodes and cables.

5.3.2.3 Placement of Electrodes Grid

A sixty-four electrode grid was placed to cover a skin portion (located from 10% to 40%) of the forearm length (measured from the lateral epicondyle to the ulnar styloid) (see **Figure5.14**). Considering the average forearm length of participated subjects is 25 cm, 10% corresponds to 2.5 cm and 40% corresponds to 10.0 cm (both from the lateral epicondyle side).

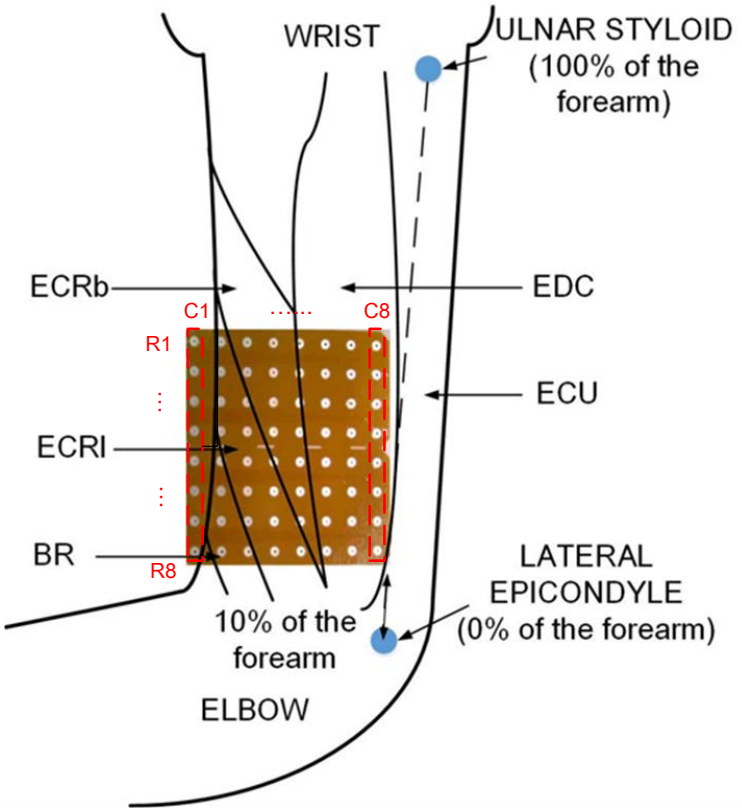

Figure5.14: The horizontal line of the sixty-four electrodes grid (8x8, 10mm IED) was placed at the 10% of the forearm, while the vertical line of the grid coincided with the line connecting the lateral epicondyle and the ulnar styloid. Lateral epicondyle near elbow is the start point (0% of the forearm length) and ulnar styloid near wrist is the end point (100% of the forearm length). The position of brachioradialis (BR), extensor carpi radialis longus (ECRl), extensor carpi radialis brevis (ECRb), extensor digitorum communis (EDC) and extensor carpi ulnaris (ECU) are also marked in this figure. C1 is column 1 (medial) and C8 is column 8 (lateral) of the electrode grid. R1 is row 1 (distal) and R8 is row 8 (proximal).

5.3.4 Experiment Connections

Connections between the subjects forearm and the prototype of multi-channel HD-sEMG recording system with wireless communication (HD-sEMG RSWC) are depicted in **Figure5.15**.

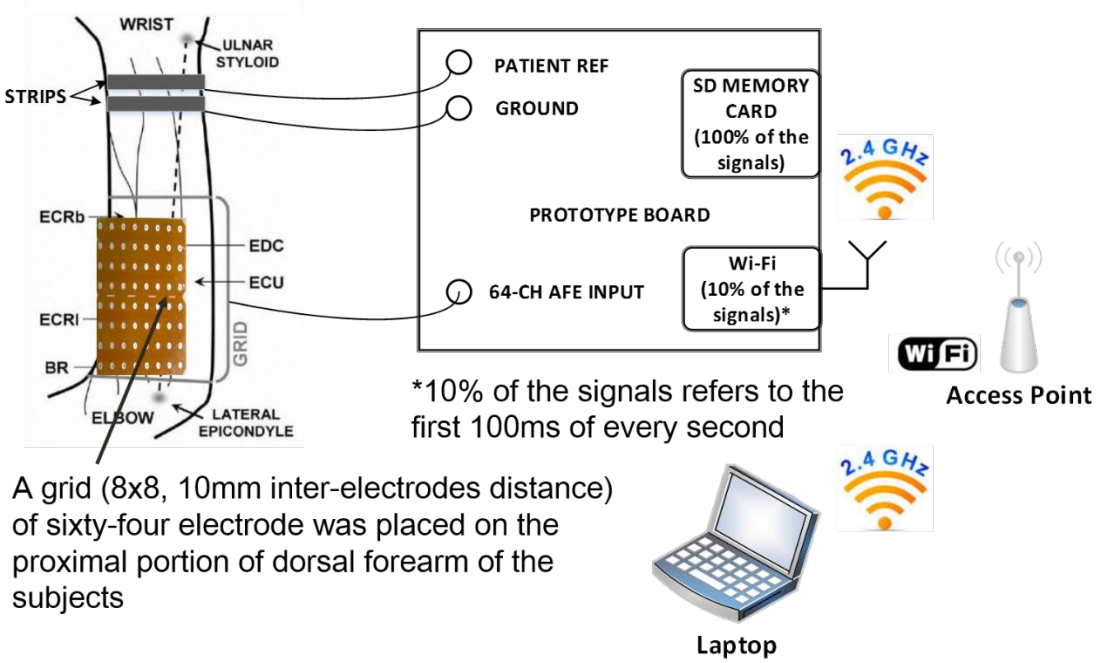

Figure5.15: Connections between the subjects forearm and the prototype of multi-channel HD-sEMG recording system with wireless communication. During the measurements, a grid of sixty-four electrodes (8x8, 10mm IED) was placed on the dorsal forearm of the subject and connected to the on-board 64-channel AFE (Analog Front End) inputs, while two strips (wetted) were also placed on the wrist separated from each other as references (patient reference and ground). The position of brachioradialis (BR), extensor carpi radialis longus (ECRl), extensor carpi radialis brevis (ECRb), extensor digitorum communis (EDC) and extensor carpi ulnaris (ECU) are also marked in this figure.

The prototype was linked to an access point wireless (radio at 2.4GHz with Wi-Fi). Sampled data were stored in a micro-SD memory card, meanwhile, a subset of 1/10th of every second (first 100ms) were transmitted to a stand-alone Wi-Fi module. A laptop (with on-line visualizing software installed) was linked to the same access point and used for on-line visualization to check EMG signals quality.

5.3.5 Experiment Procedures

Before the beginning of the experimental session, the subjects (three subjects, one female and two males) were allowed to familiarize with the experimental setup and with the tasks required for the experimental protocol. These tasks include: wrist extension (EXT), ulnar deviation (ULN), middle finger extension (MID), ring finger extension (RING) and little finger extension (LIT). The treatment of the skin and the placement of electrodes followed the European SENIAM (Surface EMG for a Non-Invasive Assessment of Muscles) standard [3].

For all the contractions, the subjects were asked to keep their right palm and fingers without contraction relaxing on a table without clenching their fingers. The forearm was pronated, in order to limit the contribution of the ECU during wrist extension. The tested contractions were (in random order): wrist extension (EXT), ulnar deviation (ULN), middle finger extension (MID), ring finger extension (RING) and little finger extension (LIT). Each of these contractions was performed for five second duration. Monopolar surface EMG signals were collected with a 64-channel electrode grid placed on the proximal dorsal portion of the forearm with 2000Hz sampling frequency.

5.3.6 Results and Discussions

Data acquired by the prototype of multi-channel HD-sEMG recording system with wireless communication were analysed with MATLAB (version 2010a). The average forearm length was 23.7±1.5 cm (mean ±standard deviation), whereas the forearm circumference in its proximal portion was 26±2 cm. **Table5.2** presents the information of the three subjects who participated in our measurements.

Table5.2: Information about the three subjects who participated in the measurement. All three subjects are dextromanuality (right-handed) and the forearm in this table refers to right forearm.

Subject	Gender	Age [year]	Height [cm]	Weight [kg]	Forearm Length [cm]	Forearm Circumference [cm]
S1	Female	28	155	56	22	24
S2	Male	25	176	90	25	28
S3	Male	32	170	63	24	26

EMG signals were acquired during 5s of these contractions and recorded in SD memory for off-line signal processing. These off-line signal processing (described in **SETCTION4.2-4.4** in detail), includes:

1) DC Removal, the DC offsets were removed from each signal after channel remapping.

2) A 2nd order digital Butterworth zero-lag band-pass (around [20, 500] Hz) filter was performed to remove the noises outside surface EMG bandwidth.

3) If 50Hz power line interference and its harmonics were detected using spectral analysis, an approach called spectrum interpolation was performed to reduce the power line interference and its harmonics (up to 10th harmonics as described in **SECTION4.4**).

4) EMG signals (monopolar) inside the epoch [1s, 4s] were extracted to calculate the RMS values of each channel and fill these values to a 2D map with a colorbar.

5) Single differential EMG signals along muscle fiber direction column by column (7 single differential signals per column) were plotted.

5) Centroids of these 2D RMS map (in step4) were used to estimate the position of the EMG source during these contractions. These 2D RMS maps were updated by replacing the RMS values below a threshold (70% of the maximal RMS value of the RMS map) with zero, in order to make a better estimation of most active region.

Single differential EMG signals of subject 3 acquired during wrist extension contraction

is presented in **Figure5.16**. Due to the fact that the 8x8 array cover more than one muscle and during each task only a small portion of the area were active, the propagation of motor unit action potential (MUAP) can only be detected clearly on column 3 (C3) and column 4 (C4).

Selection of 70% (of the maximal RMS value of the RMS map) as threshold to compute centroids of the most active area during contractions is through visual inspection among results that set 60%, 70% and 80% (of the maximal RMS value of the RMS map) as the threshold. As shown in **Figure5.18**, **Figure5.19** and **Figure5.20**, set 70% (of the maximal RMS value of the RMS map) as the threshold can select most active area properly in our experimental data.

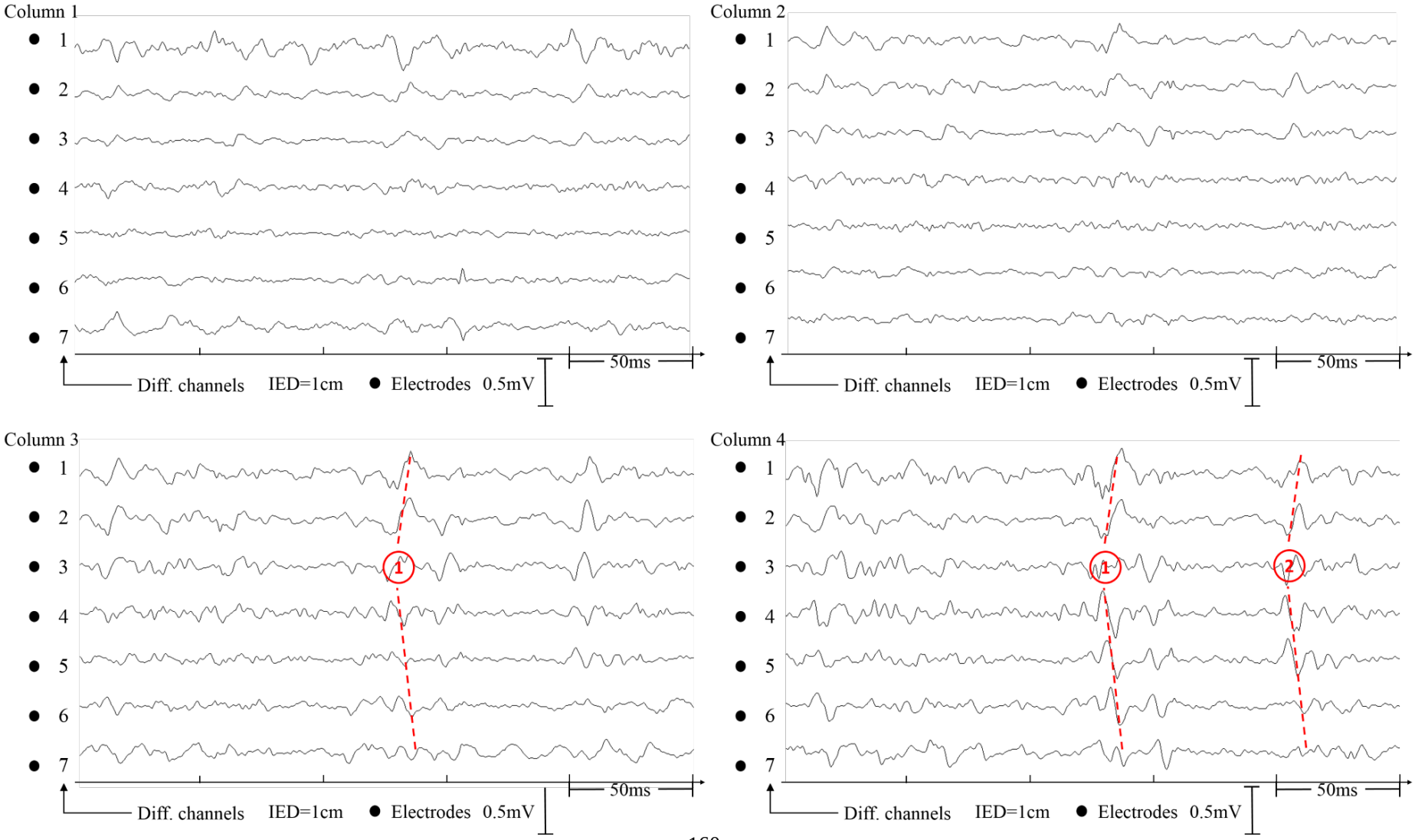
Column 1
1
2
3
4
5
6
7
50ms
Diff. channels
IED=1cm
Electrodes
0.5mV
Column 2
1
2
3
4
5
6
7
50ms
Diff. channels
IED=1cm
Electrodes
0.5mV
Column 3
1
2
3
4
5
6
7
1
50ms
Diff. channels
IED=1cm
Electrodes
0.5mV
Column 4
1
2
3
4
5
6
7
1
2
50ms
Diff. channels
IED=1cm
Electrodes
0.5mV

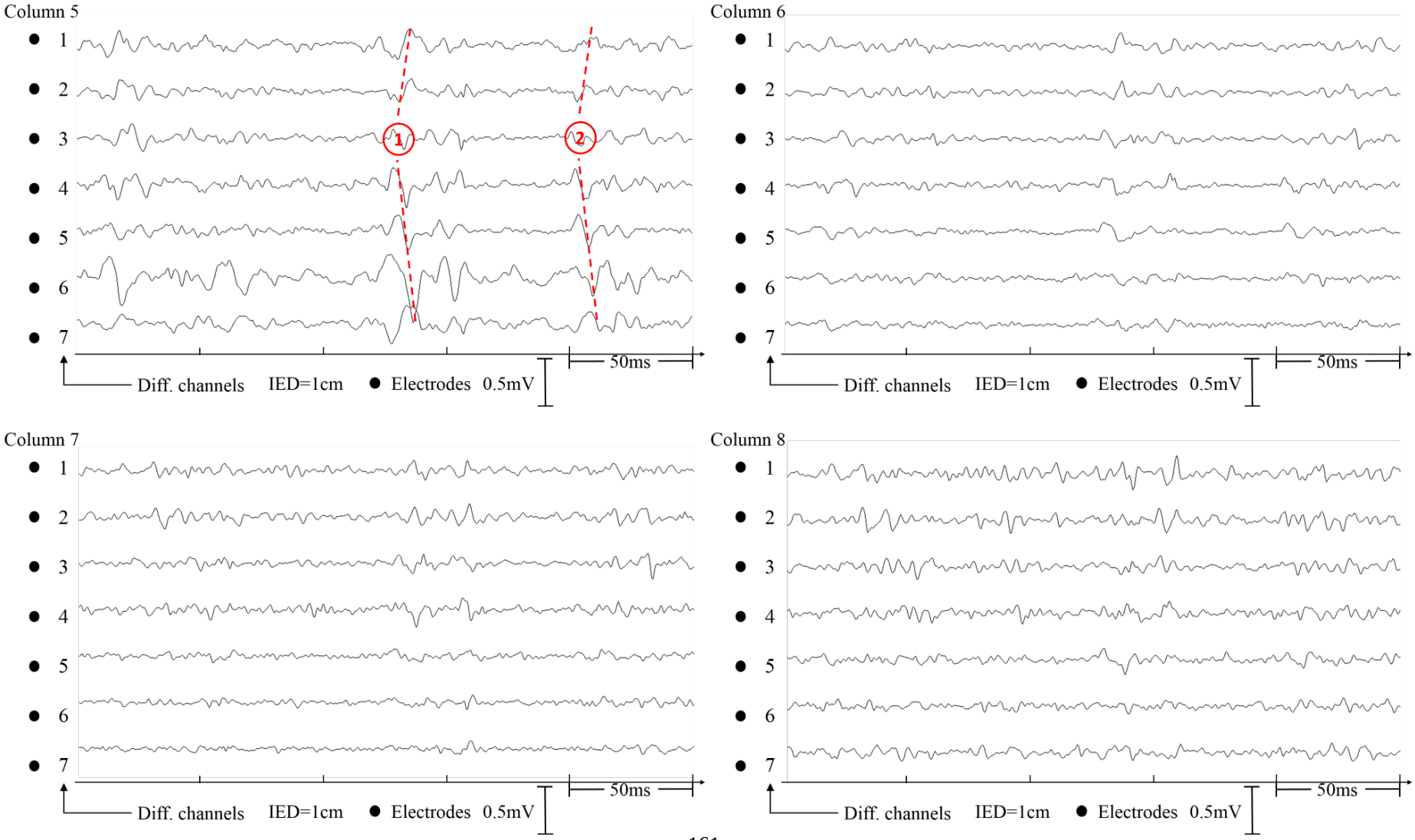
Column 5
1
2
3
4
5
6
7
1
2
50ms
Diff. channels
IED=1cm
Electrodes
0.5mV
Column 6
1
2
3
4
5
6
7
50ms
Diff. channels
IED=1cm
Electrodes
0.5mV
Column 7
1
2
3
4
5
6
7
50ms
Diff. channels
IED=1cm
Electrodes
0.5mV
Column 8
1
2
3
4
5
6
7
50ms
Diff. channels
IED=1cm
Electrodes
0.5mV

Figure5.16: Time course (over 250ms) of the EMG signals detected from each column (columns 1-8, 7 channels per column). The EMG signals are sampled at 2000 S/s (0.5ms between samples). The placement of the 64-channel electrode grid (see Figure5.14) of subject 3 (S3) during wrist extension. EMG signals are initially acquired in monopolar configuration and are converted to SD later. The propagation of MUAPs is marked with red line. Due to the fact that the 8x8 array covers more than one muscle and during each task only a small portion of the area are active, the propagation of motor unit action potential (MUAP) can only be detected on column 3-5 (a portion of extensor digitorum communis, EDC). The territory of MU1 is column 3-5 (the maximal amplitude detected in column4 and decreased to two sides). The territory of MU2 is column 4-5. The CNVs estimated (with the method presented in Figure5.7) from column 3-5 are more or less the same.

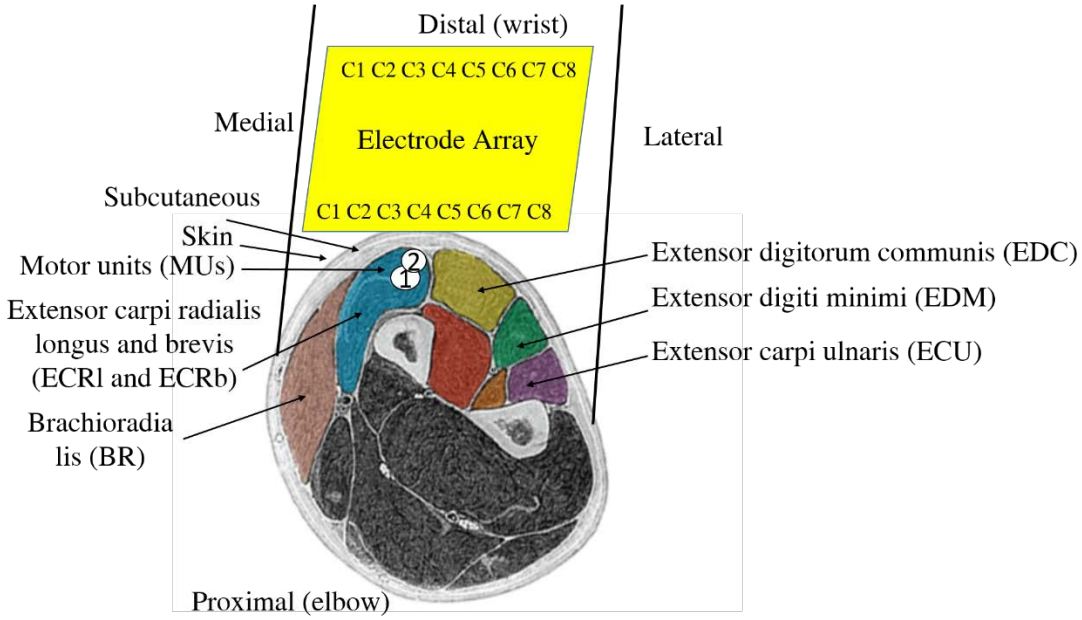

Figure5.17: Anatomical model to explain the phenomena detected in Figure5.16. The model consists of bone, muscle tissue, a subcutaneous layer and skin and MUs are simplified as several cylindrical muscle fibers cluster marked with number. Extensor carpi radialis longus and brevis (ECRl and ECRb) are considered as the muscles to generate wrist extension. The source of EMG signals is two MUs (marked with number) located in these muscles. The territory of MU1 is larger and can be detected in column 3-5. The territory of MU2 is smaller and can be detected in column 3-4. C1 is column 1 and C8 is column 8 of the electrode array.

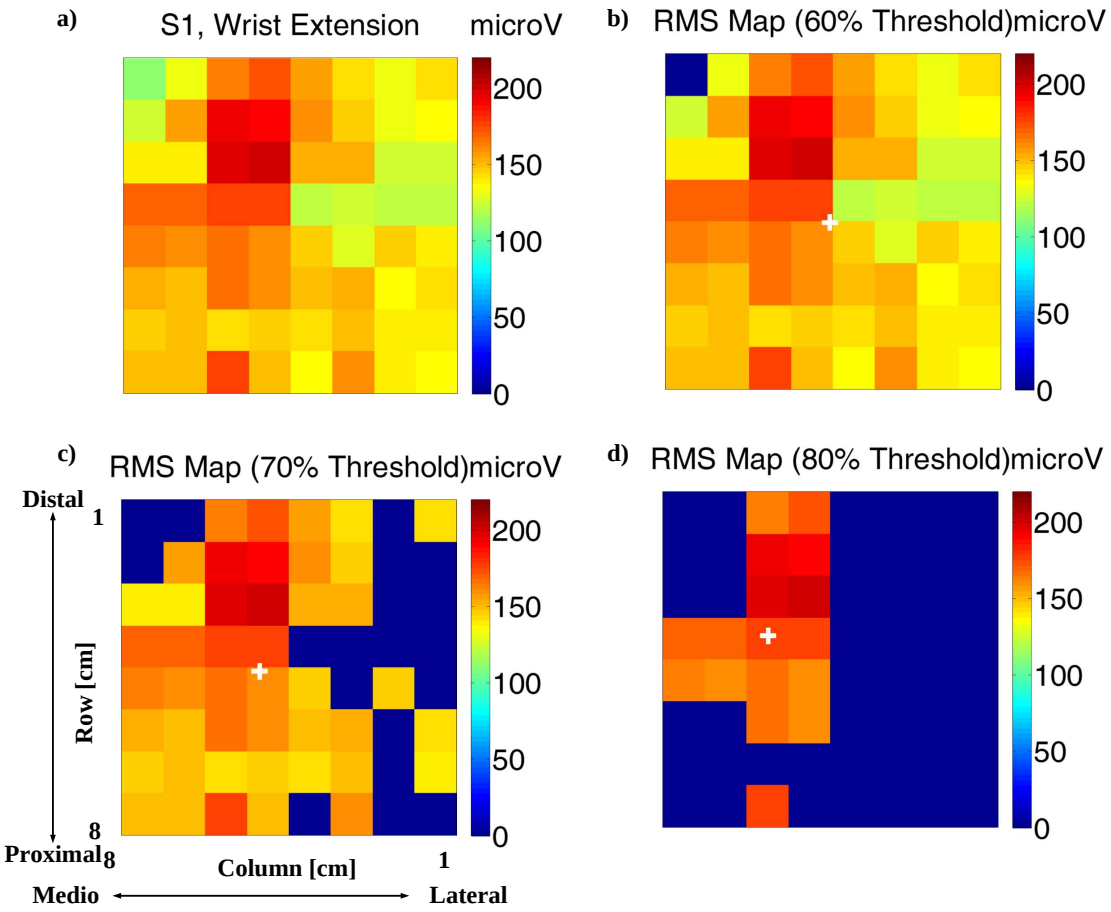

Figure5.18: Monopolar EMG amplitude distribution during wrist extension contraction of subject 1 (S1) and the positions of centroid by set 60%, 70% and 80% of the maximal RMS value of the RMS map as threshold. (a) Monopolar Surface EMG amplitude distribution (RMS) over the skin during wrist extension contraction of a representative subject (S1, subject 1). (b) The updated RMS map and its centroid by setting 60% of the maximal RMS value of the RMS map as threshold. (c) The updated RMS map and its centroid by setting 70% of the maximal RMS value of the RMS map as threshold. (d) The updated RMS map and its centroid by setting 80% of the maximal RMS value of the RMS map as threshold.

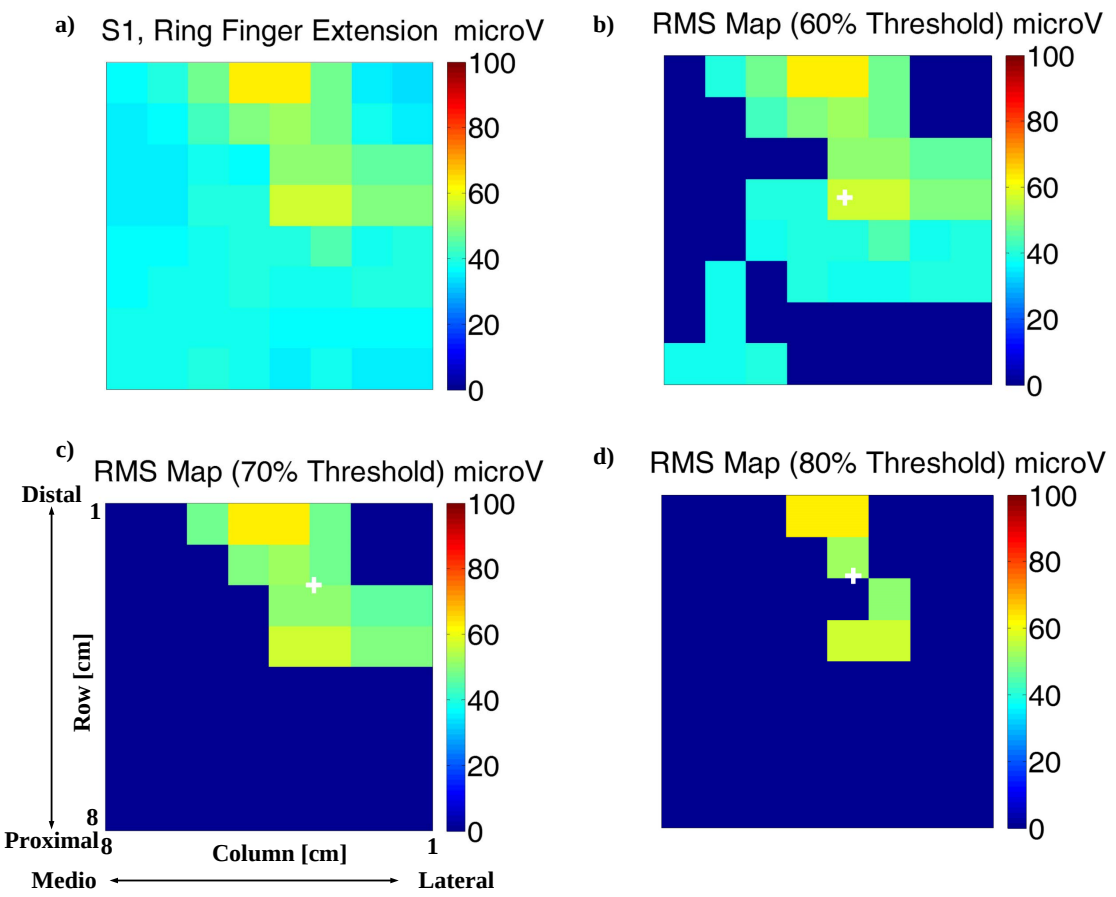

Figure5.19: Monopolar EMG amplitude distribution during ring finger extension of subject 1 (S1) and the positions of centroid by set 60%, 70% and 80% of the maximal RMS value of the RMS map as threshold. (a) Monopolar Surface EMG amplitude distribution (RMS) over the skin during ring finger extension of a representative subject (S1, subject 1). (b) The updated RMS map and its centroid by setting 60% of the maximal RMS value of the RMS map as threshold. (c) The updated RMS map and its centroid by setting 70% of the maximal RMS value of the RMS map as threshold. (d) The updated RMS map and its centroid by setting 80% of the maximal RMS value of the RMS map as threshold.

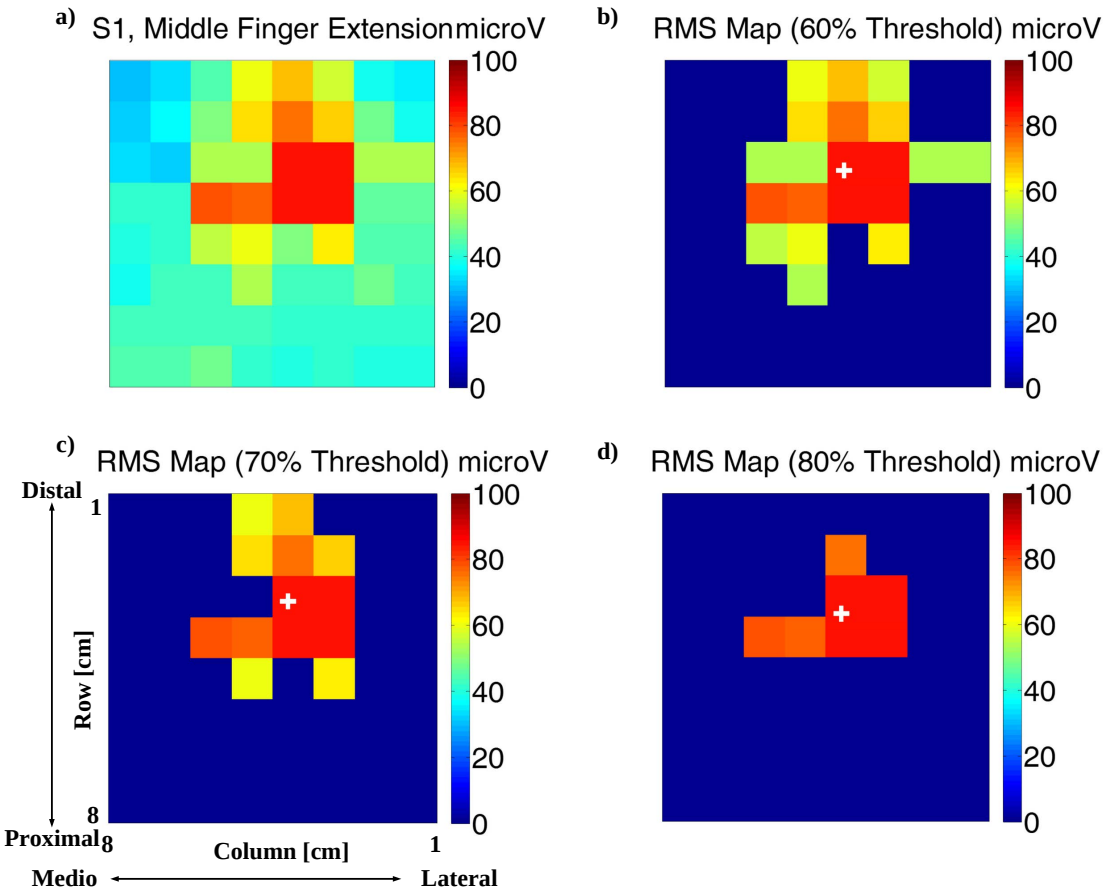

Figure5.20: Monopolar EMG amplitude distribution during middle finger extension of subject 1 (S1) and the positions of centroid by set 60%, 70% and 80% of the maximal RMS value of the RMS map as threshold. (a) Monopolar Surface EMG amplitude distribution (RMS) over the skin during middle finger extension of a representative subject (S1, subject 1). (b) The updated RMS map and its centroid by setting 60% of the maximal RMS value of the RMS map as threshold. (c) The updated RMS map and its centroid by setting 70% of the maximal RMS value of the RMS map as threshold. (d) The updated RMS map and its centroid by setting 80% of the maximal RMS value of the RMS map as threshold.

Figure5.21 presents the positions of centroid in surface EMG amplitude RMS map during different contractions [wrist extension (WRIST EXT), ulnar deviation (ULN DEV), middle finger extension (MID FINGER), ring finger extension (RING FINGER) and little finger extension (LIT FINGER)] of all three subjects.

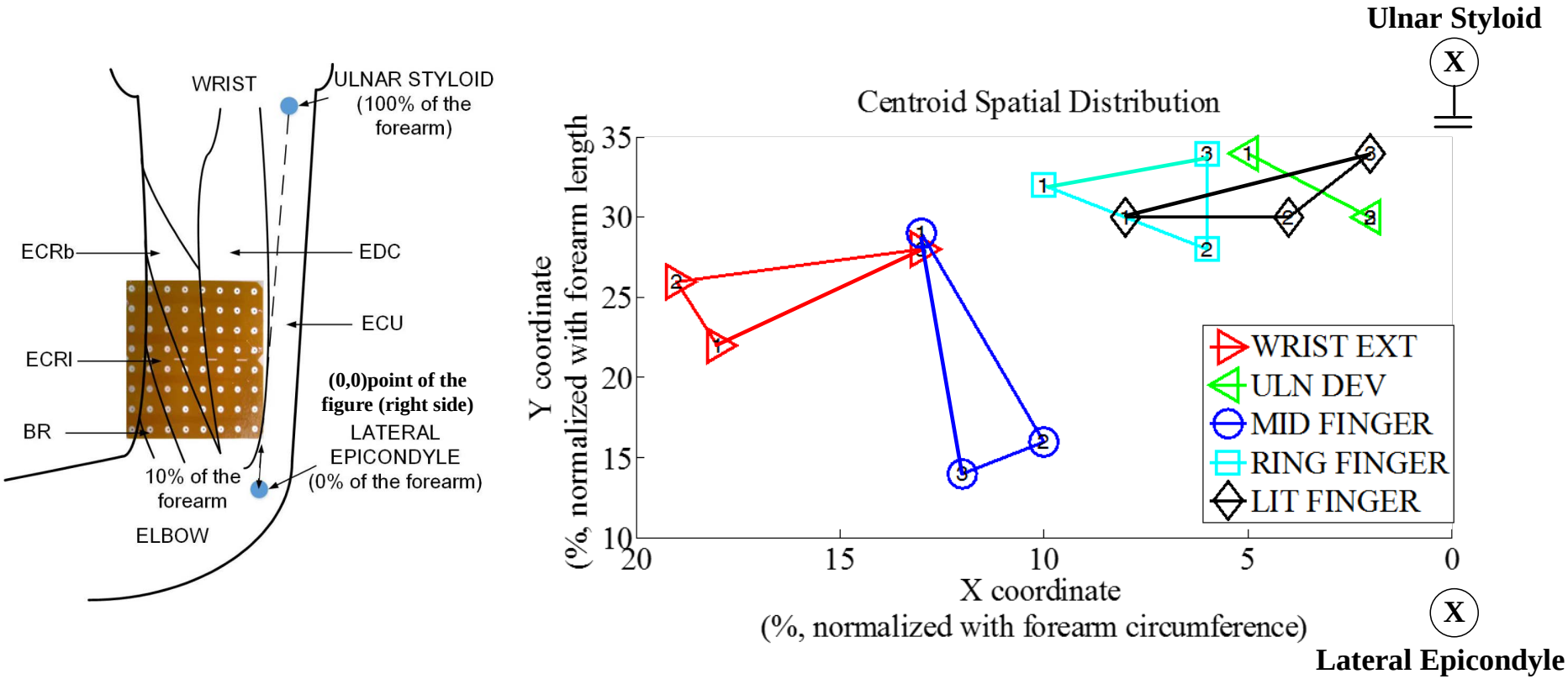

Figure5.21: Positions of the centroids (estimated the most active area) identified from EMG amplitude distributions during the contractions tested. These contractions include: wrist extension (WRIST EXT), ulnar deviation (ULN DEV), middle finger extension (MID FINGER), ring finger extension (RING FINGER) and little finger extension (LIT FINGER). Furthermore, the number "1, 2, 3" inside the mark of centroid gravity indicated that they were from subject 1, subject 2 or subject 3. The centroids of the subject 2 and 3 (ulnar deviation) are too close and it looks like only one point in the figure.

As shown in **Figure5.21**, the estimated positions (centroid gravities) of the most active area during different contractions are distinguishable. After normalization (X coordinate normalized with forearm circumference, Y coordinate normalized with forearm length), these positions from three different subjects follow a same trend. The positions of the most active area during middle finger extension have the biggest deviation, this properly due to less independence of the middle finger extension contraction compared to other contractions.

5.3.7 Conclusions

This physiological application shows that the spatial properties of monopolar EMG amplitude distribution (RMS) over the proximal portion of dorsal forearm can be used to discriminate different contractions [wrist extension (WRIST EXT), ulnar deviation (ULN DEV), middle finger extension (MID), ring finger extension (RING) and little finger extension (LIT)]. These contractions only activated a relatively small area of the proximal portion of dorsal forearm in our experiments. Experiment results also show that each contraction corresponded to a specific EMG distribution with relevantly high amplitude values in few channels only.

Reference

[1] T. Masuda, T. Sadoyama. “The Position of Innervation Zones in the Biceps Brachii Investigated by Surface Electromyography.” *Biomedical Engineering, IEEE Transactions on.*, vol. BME–32, no. 1, pp. 36–42, Jan. 1985.

[2] HowToMedia, Inc. “Muscles of Arm and Hand.” Available: http://www.innerbody.com/anatomy/muscular/arm-hand. Accessed on: Jan.15, 2015.

[3] H.J. Hermens, B. Freriks, R. Merletti. “European Recommendations for Surface ElectroMyoGraphy: Results of the SENIAM project.” 1999.

[4] Roberto Merletti and Philip J. Parker. *Electromyography: Physiology, Engineering, and Non-Invasive Applications.* Hoboken, New Jersey, USA: Wiley– IEEE Press, 2004.

[5] Marco Barbero, Roberto Merletti, Alberto Rainoldi. Atlas of Muscle Innervation Zones Understanding Surface Electromyography and Its Applications. Italy: Springer-Verlag Italia, 2012.

[6] Farina D, Mesin L, Martina S, Merletti R. “A surface EMG generation model with multilayer cylindrical description of the volume conductor.” IEEE Trans Biomed Eng., vol. 51, pp. 415–426, 2004.

[7] Dario Farina, Francesco Negro, Marco Gazzoni, Roger M. Enoka. “Detecting the Unique Representation of Motor-Unit Action Potentials in the Surface Electromyogram.” Journal of Neurophysiology, vol. 100, no. 3, pp. 1223–1233, May 2008.

[8] H. Van Duinen, W.S. Yu and S.C. Gandevia. “Limited ability to extend the digits of the human hand independently with extensor digitorum.” *J. Physiol.*, vol.15, no. 20, pp. 4799–4810, 2009.

[9] S. Riek and P. Bawa. “Recruitment of motor units in human forearm extensors.” *J. Neurophysiol.*, vol. 68, pp. 100–108, 1992

[10] M. Sagae, K. Suzuki, T. Fujita, et al. “Strict actions of the human wrist extensors: a study with an electrical neuromuscular stimulation method.” *J. Electromyogr. Kinesiol*. vol. 20, pp. 1178–1185, 2010.

[11] S. Riek, R.G. Carson and A. Wright. “A new technique for the selective recording of extensor carpi radialis longus and brevis EMG.” *J. Electromyogr. Kinesiol.*, vol. 10, pp. 249–253, 2000.

[12] R. L. Segal, P. A. Catlin, E.W. Krauss, et al. “Anatomical partitioning of three human forearm muscles.” *Cells Tissues Organs.*, vol. 170, pp. 183–197, 2002.

[13] A. Gallina, A. Botter. “Spatial localization of electromyographic amplitude distributions associated to the activation of dorsal forearm muscles.” *Frontiers in Physiology*, vol. 4, Dec. 2013.

[14] Teach me anatomy. “Muscles in the Posterior Compartment of the Forearm.” Available: http://teachmeanatomy.info/upper-limb/muscles/posterior-forearm/. Accessed on: Sep.15, 2014.

6

Discussions and Conclusions

6.1 General

This section discusses about the technical advantages/disadvantages, the limitations and the future technologies of the prototype of HD-sEMG RSWC. The technical advantages and disadvantages of the design is described in **SECTION6.2.** The limitations that discovered in the prototype are discussed in **SECTION6.3** and future technologies that may be useful for a new design are discussed in **SECTION6.4**.

6.2 Technical Advantages and Disadvantages

6.2.1 Technical Advantages

The HD-sEMG RSWC prototype satisfied the design criteria as defined in **SECTION2.2** and has some advantages over two of the most advanced commercial available multi-channel EMG detection systems as following: 32-channel Wi-Fi Trentadue EMG portable device by OT Bioelecttronica [1] and 64-channel optical fiber WEMG device [2] by LISiN.

With respect to the 32-channel Wi-Fi Trentadue EMG portable device, the HD-sEMG RSWC has the following advantages:

1) Considering the price of 10.000,00 € each 32-channel Wi-Fi Trentadue EMG portable device, the cost of the HD-sEMG RSWC protocol is much more economical (less than 1.000 €, except 64-channel AFE, which is available at LISiN).
2) Provide 64-channel EMG detection that is twice of 32-channel.

With respect to the 64-channel optical fiber WEMG device, the HD-sEMG RSWC has the following advantages:

1) Cable-free in EMG signals communication and provide more freedom in EMG measurement.
2) By using only one-single channel ADC, the cost of HD-sEMG RSWC is much less than the 64-channel WEMG system, in which 8 chips of 8-channel ADC and also higher cost MCU are used.

6.2.2 Technical Disadvantages

Although the HD-sEMG RSWC prototype satisfies the design criteria as described in **SECTION2.2** and provides good EMG signals as described in **SECTION5.2.5&5.3.6**, it still has some minor disadvantage.

With respect to the 32-channel Wi-Fi Trentadue EMG portable device, the HD-sEMG RSWC has the following technical disadvantages:

1) The size of the prototype (188 mm x 188 mm x 67 mm with enclosure) is a little large and should be reduced to make the subjects more comfortable during measurement.
2) The weight (1.2kg) of the prototype is a little heavy and shall be reduce to make the subject more comfortable.

With respect to the 64-channel WEMG detection system, the HD-sEMG RSWC has the following technical disadvantages:

1) The resolution of the HD-sEMG RSWC is 16-bit, less than 24-bit in the 64-channel WEMG detection system.
2) By using multiplexed solution with only one-channel ADC, the prototype introduces 5-6 μs delay between two adjacent channels.

6.3 Limitations

Although the HD-sEMG RSWC prototype satisfies the design criteria that described in **SECTION2.2** and provides quite good EMG signals as described in **SECTION5.2.5&5.3.6**, it still has some minor limitations as following:

1) The capacity of the rechargeable battery (2200mAh) is too small, which provides only 1 hour continuous acquisition time. It should be replaced by a higher capacity battery.
2) Stability and distance of the wireless communication. By adopting 2.1dB gain external antenna, the wireless communication of the prototype inside 5 meter has no data loss. However, the stability can be improved by using 5GHz wireless band instead of 2.4GHz. The communication distance between EMG detection system and Wi-Fi access point can also be increased by using 5GHz band, as usually there is less interference from other Wi-Fi devices in 5GHz band.
3) The prototype can only use 64-channel electrode grid for EMG signal. This generates redundancy information, when less channels (such as 32-channel) are used.
4) The prototype functions as a data logger and the txt configuration file (write into the SD card) is the only way to change configuration. Experiment with different contraction time is not convenient. User must plug in and out SD memory card to change a configuration file for each contraction time.
5) Abstract file (defined by LISiN to record the information of subject, device and measurement such as muscles) can only be added by user off-line. It is not a convenient way and may lead to wrong documentation.

Most of these limitations can be overcome by adopting new technologies that are discussed in **SECTION6.4.**

6.4 Future Technologies

The design of the HD-sEMG RSWC was proposed four years ago and it is normal to has some limitations in nowadays. By introducing the newest technologies, most of the limitations discussed in **SECTION6.3** can be overcome.

The newest 64-channel AFE RHD2164 (by Intan Techonogies) is available only in 7.3 mm x 4.2 mm x 0.2mm size [3] and provides digital output through SPI bus, which saves time and cost to add ADCs. By introducing this chip, the size and the weight of the future design will be reduced significantly. Also the time delay between two channels will disappear.

Another technology is IEEE 802.11ac [4]. It is a wireless networking standard in the 802.11 family (which is marketed under the brand name Wi-Fi), providing high-throughput wireless local area networks on the 5 GHz band. The standard was developed from 2011 through 2013 and approved in January 2014. This specification has expected multi-station WLAN throughput of at least 1 gigabit per second and a single link throughput of at least 500 megabits per second (500 Mbit/s). Working on the 5GHz band makes IEEE 802.11ac technology more stable and faster than IEEE 802.11b/g/n that used in the HD-sEMG RSWC prototype.

Reference

[1] OT Bioelettronica. “32-channel Wi-Fi Trentadue EMG portable device.” Available: http://www.otbioelettronica.it/index.php?option=com_content&view=article&id=47:trentadue&catid=18:strumentazione-portatile&Itemid=101&lang=en. Accessed on: Jan.15, 2015.

[2] Umberto Barone. “A new portable High Density Surface EMG Multichannel Acquisition System.” PhD. Thesis, Politecnico di Torino, Italy, 2013.

[3] Intan Techonogies. “RHD2164 64-Channel Amplifier Board.” Available: http://www.intantech.com/RHD2164_amp_board.html. Accessed on: Jan.15, 2015.

[4] Wikipedia. “IEEE 802.11ac.” Available: http://en.wikipedia.org/wiki/IEEE_802.11ac. Accessed on: Jan.15, 2015.